

Trans-Relativistic Blast Waves in Supernovae as Gamma-Ray Burst Progenitors

Jonathan C. Tan¹, Christopher D. Matzner², and Christopher F. McKee^{1,3}

1. *Department of Astronomy, University of California, Berkeley, CA 94720, USA.*

2. *CITA, University of Toronto, 60 St. George Street Toronto, Ontario M5S 3H8, Canada.*

3. *Department of Physics, University of California, Berkeley, CA 94720, USA.*

ABSTRACT

We investigate the acceleration of shock waves to relativistic velocities in the outer layers of exploding stars. By concentrating the energy of the explosion in the outermost ejecta, such trans-relativistic blast waves can serve as the progenitors of gamma-ray bursts (GRBs); in particular, the “baryon-loading” problem that plagues many models of GRBs is circumvented. Postshock acceleration is effective in boosting the kinetic energy in relativistic ejecta. We present physically motivated analytic expressions to describe trans-relativistic blast waves in supernovae, and we validate these expressions against numerical simulations of test problems. Investigating the effect of stellar structure on mass ejection, we find that relativistic ejecta are enhanced in more centrally condensed envelopes—e.g., for radiative envelopes, when the luminosity approaches the Eddington limit. Convenient formulae are presented with which to estimate the production of relativistic ejecta from a given progenitor.

We apply our analytic and numerical methods to a model of SN 1998bw, finding significantly enhanced relativistic ejecta compared to previous studies. We propose that GRB 980425 is associated with SN 1998bw and may have resulted from an approximately spherical explosion producing $\sim 10^{-6} M_{\odot}$ of mildly relativistic ejecta with mean Lorentz factor $\bar{\Gamma} \sim 2$, which then interacted with a dense circumstellar wind with mass loss rate $\sim \text{few} \times 10^{-4} M_{\odot} \text{ yr}^{-1}$. A highly asymmetric explosion is not required. An extreme model of “hypernova” explosions in massive stars is able to account for the energetics and relativistic ejecta velocities required by many of the observed cosmological GRBs. However, the most energetic bursts require asymmetric expulsion of ejecta, perhaps caused by rotationally flattened progenitors. We present simplified models and simulations of explosions resulting from accretion-induced collapse of white dwarfs and phase transitions of neutron stars. While we find increased energies in relativistic ejecta compared to previous studies, these explosions are unlikely to be observed at cosmological distances with current detectors, unless extreme explosion energies and asymmetries are invoked.

Subject headings: gamma rays: bursts — hydrodynamics — shock waves — relativity — supernovae: individual (SN 1998bw) — stars: white dwarf, neutron

1. Introduction

More than 30 years after their discovery, gamma-ray bursts (GRBs) remain one of the most outstanding puzzles in astrophysics. A “relativistic fireball” model has emerged to explain the γ -ray emission and successfully predict the existence of longer wavelength afterglows. How-

ever, the identity, or identities, of the central engine driving such fireballs is literally shrouded in uncertainty. At least two major problems stalk the proposed GRB models. Firstly, extreme isotropic energies are implied by the cosmological distances of some bursts, determined from redshifted absorption lines in their afterglows. Secondly, the “baryon loading - compactness prob-

lem” results from the large energies, small sizes (implied by short timescale variability) and optically thin spectra of GRBs and requires the source to move towards us highly relativistically. This in turn mandates miniscule mass-loading, $\sim 5.6 \times 10^{-5} E_{\gamma,52} (\bar{\Gamma}/100)^{-1} \epsilon_{\gamma}^{-1} M_{\odot}$, where $E_{\gamma,52}$ is the isotropic γ -ray energy in units of 10^{52} ergs, $\bar{\Gamma} \equiv (1 - \bar{\beta}^2)^{-1/2}$ is the mean Lorentz factor of the source mass ($\bar{\beta}$ is the mean velocity relative to the speed of light) and ϵ_{γ} is the conversion efficiency of bulk kinetic energy to γ -rays (see, e.g., Piran 1999, for a review).

One mechanism that can naturally overcome these hurdles is the acceleration of shocks in a progenitor, which confines and efficiently taps the energy from a central explosion resulting from the formation of a compact stellar mass object. Although the shock is initially non- or mildly relativistic, it may accelerate to relativistic velocities and channel a fraction of the total explosion energy into relativistic ejecta. Shock acceleration¹ occurs in the presence of a steeply declining density gradient, and so only a small fraction of the ejecta mass reaches relativistic speeds.

This mechanism has provided the basis for many different models of GRBs, ranging from normal supernovae (in the first astrophysical GRB model; Colgate 1974), to extremely energetic supernovae or “hypernovae” (Paczynski 1998), to phase transitions of neutron stars into strange stars (Fryer & Woosley 1998). Accretion-induced collapse of white dwarfs to neutron stars (Woosley & Baron 1992; Fryer et al. 1999) may also drive a shock into the outer atmosphere of the white dwarf, but such shocks have so far been examined only in the context of much weaker Type Ia supernova explosions (Berezinsky et al. 1996). Shock acceleration is also an important factor in aspherical models such as those involving rotationally flattened progenitors (Chevalier & Soker 1989; Khokhlov et al. 1999) and jet-like explosions of the core (MacFadyen & Woosley 1999; Höflich et al. 1999). Even if a jet pierces the stellar envelope entirely (as in the model of Aloy et al. 2000), the production of relativistic ejecta by shock acceleration may dominate the observed GRB in most

¹We shall use the term “shock acceleration” to refer to this hydrodynamical effect, which ought not be confused with particle acceleration in shocks.

directions.

While the propagation of shock waves is well understood in the nonrelativistic (Sedov 1946, 1959; Taylor 1950; Ostriker & McKee 1988; Matzner & McKee 1999) and ultrarelativistic (Johnson & McKee 1971; Blandford & McKee 1976) regimes, similarity solutions do not exist for the mildly relativistic case. Thus, previous analytic models of the acceleration of shocks at these intermediate velocities have extrapolated non-relativistic results with simple scaling laws (e.g. Gnatyk 1985) intermediate between the non- and ultrarelativistic limits. Furthermore, the post-shock evolution of trans-relativistic ejecta has received only a crude treatment, if any, in previous work.

The aim of this paper is to provide a quantitative, theoretical description of trans-relativistic shock and postshock acceleration, which will be of use in many GRB models. A *trans-relativistic blast wave* is one in which some of the mass is accelerated to highly relativistic velocities, but most of the mass is not; in particular the ratio of the explosion energy to the rest energy of the ejecta is $< \mathcal{O}(1)$. In §2, utilizing a relativistic one-dimensional Lagrangian hydrodynamic code based on the method of exact Riemann solvers (Martí & Müller 1994), we investigate the dynamics of shocks and shocked ejecta in idealized model density distributions. We present physically motivated analytic approximations to describe the shock and postshock acceleration as well as the kinetic energy distribution of ejecta from density distributions approximating polytropes at their edges. We explore how a progenitor’s structure affects its ejecta in §2.4, finding that highly condensed envelopes produce fast or relativistic ejecta most efficiently and that this corresponds to stars whose luminosities approach the Eddington limit. We present formulae to estimate the energy in relativistic ejecta from the parameters of a given progenitor star. Our results, although primarily derived for spherically symmetric explosions, can also be applied to sectors of aspherical explosions, a topic we address in §2.5. Explosions where the effect of gravity is strong, for example relevant to ejecta from neutron stars, are treated in §2.6.

We apply our results to four astrophysical examples, as potential GRB engines (§3). First, and in most detail, we consider supernova explosions in

the exposed cores of massive post main-sequence stars (§3.1). The probable association of supernova (SN) 1998bw with GRB 980425 (Galama et al. 1998) has sparked renewed interest in such models. Other supernovae for which a suspicion of GRB association exists include SN 1997cy with GRB 970514 (Germany et al. 2000; Turatto et al. 2000) and SN 1999E with GRB 980901 (Thorsett & Hogg 1999). The late time excess flux, relative to that expected from a power-law decline, of the afterglows of GRB 970228 (Fruchter et al. 1999) and GRB 980326 (Bloom et al. 1999) has been cited as evidence for the presence of supernovae (Bloom et al. 1999; Reichart 1999; Galama et al. 2000). However, alternative mechanisms of afterglow re-radiation (Waxman & Draine 2000) and scattering (Esin & Blandford 2000) by dust, have also been proposed to produce the excess flux. Cosmological GRB afterglows are associated with the stellar population of their host galaxies (Bloom et al. 2000b), but there is only tentative evidence for a direct association with star forming regions (Kulkarni et al. 2000; Djorgovski, Bloom, & Kulkarni 2000; Galama & Wijers 2000), which would be expected if they arose from the deaths of massive stars.

If there is an association between GRB 980425 and SN 1998bw, then the γ -ray energy is only $\sim 10^{48}$ ergs, thousands to millions of times weaker than the inferred isotropic energies of the cosmological bursts; moreover, its associated galaxy is much too near to be drawn from the same distribution as the other known host galaxies (Hogg & Fruchter 1999). This event may be an example of a subclass of GRBs, termed S-GRBs (Bloom et al. 1998a). Woosley et al. (1999) simulated an energetic ($\sim \text{few} \times 10^{52}$ ergs) explosion in a variety of carbon-oxygen and helium star progenitors, attempting to fit the observed supernova lightcurve. They considered the possibilities of γ -ray emission from shock break-out and the interaction of ejecta with a circumstellar wind. With non-relativistic codes they found the simple spherical case unable to produce enough relativistic ejecta to account for even this weak GRB. This result, together with the extremely large isotropic energies ($E_\gamma \sim 10^{51} - 10^{54}$ ergs) of the cosmological bursts, has focussed attention on aspherical explosions involving jets, which may be able to explain the different types of GRBs as a func-

tion of the viewing angle to the jet (Wheeler et al. 2000a,b; MacFadyen & Woosley 1999; MacFadyen et al. 2000; Aloy et al. 2000; Wang et al. 2000). However, uncertainties in previous models of trans-relativistic dynamics warrant further investigation of the simplest spherical case. Indeed, our relativistic analysis of the model considered by Woosley et al. (1999) yields sufficient mildly relativistic ejecta to account for GRB 980425 and radio observations of SN 1998bw, for a progenitor embedded in a dense wind with mass loss rate $\sim \text{few} \times 10^{-4} M_\odot \text{ yr}^{-1}$. Our analysis therefore validates the suggestion by Matzner & McKee (1999) that GRB 980425 could be the product of a *spherical* explosion of SN 1998bw.

In §3.2 we continue with explosions in the cores of massive stars, but now at much greater energies. These hypernovae² are hypothesized to result from magnetic extraction of the rotational energy of nascent neutron stars or black holes (Paczynski 1998). We consider an extreme example with 5×10^{54} ergs, which might arise from the formation of a $\sim 10 M_\odot$ black hole. For the purposes of this crude estimate, we embed the explosion in the $\sim 5 M_\odot$ envelope ejected from our SN 1998bw progenitor, and calculate the resulting energy distribution. To compare to the observed cosmological bursts we derive conservative constraints on the minimum mean Lorentz factor of ejecta carrying the γ -ray energy, by considering the timescale of the burst, and requiring the implied circumstellar material to be optically thin to the burst photons. We also consider the minimum Lorentz factor required for the optical depth due to photon-photon pair production to be small. We find that the overall energetics and relativistic ejecta velocities required by many cosmological bursts can be explained by such a simple, though admittedly extreme, model. However there are some events, notably GRB 990123, that lie well beyond the reach of the spherical model. Considering aspherical explosions (§2.5), we calculate that enhancements in shock strength along the preferred axis, perhaps set by rotation, by factors of only a few are required to explain all cosmological GRBs. Interaction of the relativistic ejecta with inhomogeneities may give bursts some short timescale substructure

²Unlike Iwamoto et al. (1998), we shall reserve the term “hypernovae” for much more energetic events than SN 1998bw.

(Dermer & Mitman 1999; Fenimore et al. 1999), though this can only account for a small fraction of the total burst energy (Sari & Piran 1997). Instabilities associated with an accelerating shock (Luo & Chevalier 1994) may create postshock velocity perturbations that also lead to GRB variability.

Finally we consider simple models of explosions in white dwarfs and neutron stars (§3.3), in order to investigate shock and postshock acceleration in their outer layers. Such shocks may be driven by the accretion-induced collapse of a white dwarf to a neutron star or the phase transition of a neutron star to a hypothesized “strange” star, composed of more stable strange quark matter. For the production of relativistic ejecta, these models have the advantage that large explosion energies may be coupled to very small ejecta masses. Given a total ejecta mass and energy, as predicted from detailed core-collapse models (Fryer & Woosley 1998; Fryer et al. 1999), we estimate the energy distribution of the ejecta. Again, we find enhanced amounts of energy in relativistic ejecta compared to previous estimates. We compare to cosmological GRBs, this time by combining the burst timescale with an assumed density of a uniform ambient medium. We find that white dwarf explosions are unlikely to be relevant to these bursts. Our neutron star models, while more energetic, need to be pushed to extreme limits to provide observable fluxes at cosmological distances.

2. Theory

The process of mass ejection in a supernova explosion proceeds in a sequence of distinct dynamical phases (Matzner & McKee 1999). In the first phase, the stellar envelope is engulfed by the outward-propagating blast wave launched by collapse of the core. Except perhaps in the vicinity of the central engine and within the shock itself, the blast wave is adiabatic. For an explosion in the tenuous outer envelope of a supernova, the postshock pressure is dominated by photons; for a relativistic shock in a compact object, it may be dominated by relativistic motions of leptons (Weaver 1976). In either case, the ratio of specific heats is $\hat{\gamma} = 4/3$. The boundary of this blast wave is a shock front, which imprints its velocity (and an associated specific entropy) on the postshock gas. The shock velocity decreases in most parts of the

star, but it increases in regions with a sufficiently steep density profile – an effect analogous to the cracking of a whip. As the postshock pressure is dominated by radiation pressure, the shock front has a finite optical depth (for which photons diffuse upstream as fast as gas flows downstream). Thus the shock breaks out of the star at some finite depth. Only for a sufficiently energetic explosion in a sufficiently compact star will the shock accelerate to relativistic velocities before it breaks out. In §2.1 we investigate shock acceleration in such progenitors.

After the stellar envelope has been shocked, its thermal and kinetic energies are approximately equal. The next phase of evolution is one of postshock acceleration, in which heat is converted into outward motion and the ejecta approach a state of free expansion. For the gas in the outer layers of the star, this increases the velocity by over a factor of two compared to the postshock state if the shock is nonrelativistic (Matzner & McKee 1999). However, gas hit by a relativistic shock undergoes even more dramatic acceleration, because postshock kinetic and thermal energy densities are both dominated by photons, which eventually transfer their energy to the baryons in the freely expanding state. This conversion of internal energy to kinetic leads to a large increase in the Lorentz factor during the acceleration phase. The acceleration is accentuated by the fact that each gas element is pushed outward by interior ejecta, which though slower, are at higher pressure (§2.2).

Each stage of this process has been the study of previous theoretical investigations; our goal is to investigate in greater detail the connection between the shock velocity and the final expansion velocity, across the transition from Newtonian to relativistic motion. To describe this process analytically, we present formulae that have been calibrated against numerical simulations for a variety of progenitor stars (§§2.1 and 2.2). In §2.3 we give an analytical prediction of the distribution of energy with Lorentz factor in the state of free expansion, i.e., the information necessary to calculate the circumstellar interaction and the resulting burst of energetic radiation. We consider the dependence of relativistic mass ejection on the progenitor’s structure in §2.4. We apply our dynamical results to sectors of aspherical explosions in §2.5 and explosions where the ejecta are strongly

affected by gravity in §2.6.

2.1. Shock Propagation

The propagation of a nonrelativistic blast wave through the stellar interior and the subsequent acceleration phase were studied in detail by Matzner & McKee (1999). The shock velocity, $\beta_s c$, responds to two competing trends. First is the overall deceleration as mass is entrained through the shock, $\beta_s \propto [\tilde{E}_{\text{in}}/\tilde{m}(r)]^{1/2}$, where

$$\tilde{m}(r) \equiv \frac{m(r) - M_{\text{rem}}}{M_{\text{ej}}}; \quad 0 \leq \tilde{m} \leq 1 \quad (1)$$

is the fraction of the total ejecta mass, M_{ej} , within r (excluding any remnant mass M_{rem}), and

$$\tilde{E}_{\text{in}} \equiv \frac{E_{\text{in}}}{M_{\text{ej}}c^2} \quad (2)$$

is the injected energy in units of the rest energy, which is $< \mathcal{O}(1)$ for trans-relativistic explosions. Second is the acceleration of the shock front down the declining density gradient, for which $\beta_s \propto [\tilde{m}(r)M_{\text{ej}}/(\rho r^3)]^{\alpha_{\text{nr}}}$ where $\alpha_{\text{nr}} \simeq 0.19$ for typical outer density distributions (Sakurai 1960). The shock propagation is a combination of these two trends, and it is not surprising that a product of the two formulae yields an excellent approximation to the shock velocity (Matzner & McKee 1999):

$$\beta_s = A \left(\frac{\tilde{E}_{\text{in}}}{\tilde{m}} \right)^{1/2} \left(\frac{\tilde{m}M_{\text{ej}}}{\rho r^3} \right)^{\alpha_{\text{nr}}}. \quad (3)$$

The coefficient A can be evaluated for a spherical Sedov blast wave in the distribution $\rho \propto r^{-k_\rho}$, in which it takes the value

$$A = \sigma^{-1/2} \left(\frac{4\pi}{3 - k_\rho} \right)^{-\alpha_{\text{nr}}}, \quad (4)$$

where $\sigma \equiv \tilde{E}_{\text{in}}/(\tilde{m}\beta_s^2)$, constant for self-similar blast waves, measures the fraction of the explosion energy that is kinetic. Note that the shock accelerates in this region only if $k_\rho > 3$. Matzner & McKee (1999) found that the Primakoff distribution $k_\rho = 17/7$ (for which $A = 0.794$) adequately describes the interiors of red and blue supergiant progenitors of type II supernovae. However, we have found that the accuracy of equation (3) is enhanced if A is evaluated for the typical value of k_ρ

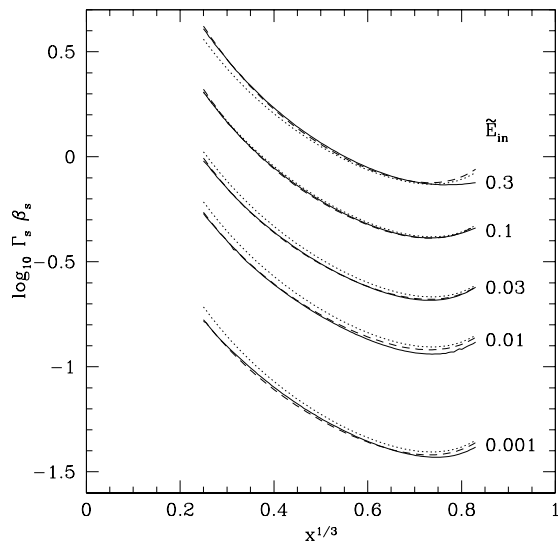


Fig. 1.— Spherical shock propagation down a density profile $\rho = \rho_h x^3$, where $x \equiv 1 - r/R$, for different explosion energies, \tilde{E}_{in} . Simulation results (*solid* lines) are compared to the analytic prediction of this paper (eqs. [14] and [15]) (*dashed* lines), and to the variation of the scaling predicted by Gnatyk (1985) (GMM scaling) as expressed by equation (9) (*dotted* lines). The normalization constant, A , is 0.68 for $\tilde{E}_{\text{in}} \leq 0.03$, and 0.72, 0.74 for $\tilde{E}_{\text{in}} = 0.1, 0.3$, respectively.

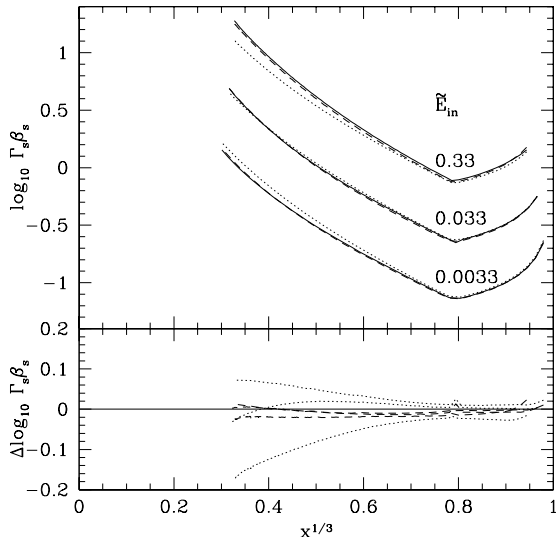


Fig. 2.— Spherical shock propagation down a realistic stellar density profile, given by equation (11). The differences between the GMM scaling (eq. [9]) (*dotted* lines) and our improved formula (eqs. [14] and [15]) (*dashed* lines) are clearly revealed in the outer region ($x^{1/3} < 0.8$), where the density gradient is very steep. The simulation results are again shown by the *solid* lines. The normalization constant, A , is 0.736 for all energies. The lower panel shows the ratio of the analytic predictions to the numerical results. For both cases $\tilde{E}_{\text{in}} = 0.0033, 0.03, 0.3$ from top to bottom. The GMM scaling under predicts relativistic shock acceleration and over-predicts nonrelativistic. The final Lorentz factor of ejecta depend sensitively on Γ_s (§2.2), and the observed difference, $\sim 33\%$, between the two laws results in a difference of a factor of ~ 3 in final Lorentz factors.

in the interior of progenitor. To make this evaluation, we use the pressure gradient approximation of Ostriker & McKee (1988), with $\hat{\gamma} = 4/3$:

$$\sigma \simeq \frac{2(29 - 7k_\rho)(3 - k_\rho)}{113 - 35k_\rho}, \quad (5)$$

which is exact for the Primakoff blast wave, $k_\rho = 17/7$. For the progenitor model CO6 of Woosley et al. (1999), which we use to simulate SN 1998bw (§3.1), we estimate $k_\rho \simeq 1.9$ which gives $A \simeq 0.736$.

We also consider the velocity normalization for shocks that develop in centrally concentrated, non-power-law distributions, with monotonically steepening density gradients as $r \rightarrow R$. These types of distribution mimic those of white dwarfs and neutron stars. We estimate a mean k_ρ in the central region, where the shock structure forms, by evaluating a moment of the whole density distribution, $J_l \equiv \int_0^R (r/R)^l d(m/M)$. For a power law distribution

$$k_\rho = \frac{(3+l)J_l - 3}{J_l - 1}. \quad (6)$$

From numerical simulation (below), we find $l = -1$ gives an estimate of an effective k_ρ which accurately predicts A , via equations (4) and (5), for $\tilde{E}_{\text{in}} \ll 1$, in several different distributions we have tested. We find A may have a weak energy dependence for $\tilde{E}_{\text{in}} \sim \mathcal{O}(1)$ (below).

Although equation (3) is quite accurate in the nonrelativistic regime, it breaks down when $\beta_s \rightarrow 1$ and the shock becomes trans-relativistic. Even in the context of a planar, power-law density distribution, the dynamics are not self-similar in this stage. Therefore, it has received little attention in previous work, whereas the opposite limit of self-similar, ultrarelativistic shock propagation was treated approximately by Johnson & McKee (1971). However, a knowledge of the nonrelativistic and ultrarelativistic shock velocity scalings does not suffice to specify the relative coefficient connecting the two stages. Moreover, it does not allow one to describe ejecta that are only mildly relativistic; as we shall show, these trans-relativistic ejecta contain more energy than the ultrarelativistic. For these reasons, we wish to investigate in detail the transition between Newtonian and ultrarelativistic motion.

Using an approximate treatment, Johnson & McKee (1971) presented the following estimate of the shock Lorentz factor, $\Gamma_s \equiv (1 - \beta_s^2)^{-1/2}$, valid in the ultrarelativistic ($\Gamma_s \gg 1$) limit:

$$\Gamma_s \simeq \frac{1}{\sqrt{2}} \left(\frac{E_i}{\rho c^2} \right)^{\alpha_r}, \quad (7)$$

where $\alpha_r = \frac{1}{2}\sqrt{3}(2 + \sqrt{3})^{-1} \simeq 0.232$, and E_i is the energy density at some reference point in the flow. Johnson & McKee obtained this result by assuming that initially a region of hot gas, with a spatially uniform value of E_i , abutted cold gas with decreasing density $\rho(r)$. As a result, the Riemann invariant was the same on all forward characteristics emanating from the hot gas. In the case considered here there is no region with constant E_i , so the exact values of α_r and the numerical coefficient may be somewhat different.

Noting the similarity between the Newtonian and relativistic indices α_r and α_{nr} that relate the shock velocity to the density profile, Gnatyk (1985) suggested the following formula for shocks bounding spherical blast waves:

$$\Gamma_s \beta_s \propto (\rho r^3)^{-\alpha_g}, \quad (8)$$

where $\alpha_g \simeq 0.5$ for decelerating and 0.2 for accelerating shocks. This approximation was found to be inferior to equation (3) in the nonrelativistic limit by Matzner & McKee (1999), but it does suggest that the quantity $\Gamma_s \beta_s$ can be approximated analytically.

However, equation (8) does not specify the normalization of the shock velocity. We therefore consider instead the following formula:

$$(\Gamma_s \beta_s)_{\text{GMM}} = A \left(\frac{\tilde{E}_{\text{in}}}{\tilde{m}} \right)^{1/2} \left(\frac{\tilde{m} M_{\text{ej}}}{\rho r^3} \right)^{\alpha_g}. \quad (9)$$

In the Newtonian limit this formula reduces to a shock velocity approximation very similar to equation (3), and it makes a transition to relativistic motion in the manner suggested by Gnatyk (1985), (equation [8]): hence the subscript GMM. Since $\tilde{m} \simeq 1$ in the region of strong acceleration at the outside of a star, this formula has the same scaling as equation (8) there. Whereas Woosley et al. (1999) chose the shock-velocity coefficient numerically, equation (9) uses our earlier results and those of Matzner & McKee (1999) to prescribe it

analytically. Note that it is Gnatyk’s exponent $\alpha_g = 0.2$, rather than $\alpha_{nr} = 0.19$, that enters this expression. Insofar as equation (3) accurately predicts the behavior of a nonrelativistic shock front with $\alpha_{nr} = 0.2$ (and we find that it does), equation (9) represents the result of an extrapolation to relativistic velocities using Gnatyk’s scaling. It remains to be determined whether the transition to relativistic motion is captured accurately by this formula.

To study the dynamics of trans-relativistic blast waves, we have developed a relativistic, one-dimensional Lagrangian hydrodynamics code based on an exact Riemann solver (Martí & Müller 1994). The Lagrangian nature of our code is a key requirement for handling large ranges in density with fine zoning, of particular relevance for simulating shocks accelerating in stellar atmospheres. The code accurately handles standard test problems, including Centrella’s (1986) proposed wall shock and Riemann shock tube tests. Additionally the code recovers the ultrarelativistic Blandford-McKee (1976) solution for spherical blast waves.

With this code we have conducted a suite of numerical calculations. For much of this study we employ a “stellar” model density distribution: an outer stellar envelope of polytropic index n has the density profile

$$\rho = \rho_h (R/r - 1)^n, \quad (10)$$

in any region where the external mass m_{ex} can be ignored compared to M_\star and where n does not vary. If this region extends inward to half the radius (e.g., for polytropes with $n \geq 3$; Chandrasekhar 1939) then the coefficient ρ_h is equal to the density there: $\rho_h = \rho(r = R/2)$. For our stellar model, we join this outer profile to an inner, power-law density distribution:

$$\rho = \rho_h \times \begin{cases} \left(\frac{R}{r_c} - 1 \right)^n \left(\frac{r}{r_c} \right)^{-k_\rho}, & r < r_c \\ \left(\frac{R}{r} - 1 \right)^n, & r_c < r < R. \end{cases} \quad (11)$$

We choose a core radius $r_c \simeq R/2$, polytropic index $n = 3.85$, and power law index $k_\rho = 1.9$ to resemble the progenitor model for SN 1998bw considered in § 3.1. In order to find analytical formulae valid for various density distributions, we have additionally considered an “external power law envelope” model,

$$\rho = \rho_h x^n, \quad (12)$$

also with $n = 3$, where

$$x \equiv 1 - \frac{r}{R}. \quad (13)$$

Equation (12) is the $x \rightarrow 0$ limit of the polytropic profile (10), but significantly underestimates ρ in the interior (e.g., by a factor of 2^n at $x = 1/2$).

After an injection of thermal energy in the central few zones, a shock develops and propagates outwards, decelerating in the inner region, where the density gradient is shallow, and accelerating in the outer layers, where the density gradient is steep. We have investigated explosions with \tilde{E}_{in} ranging from 0.001 to 0.33. In each case, the resolution was increased either until the numerical results converged, or until a correction for incomplete convergence could be ascertained.

Empirically, we find that the scaling proposed by Gnatyk (1985), as realized in equation (9), is roughly correct but not sufficiently accurate for a study of the energetics of relativistic ejecta. In order to capture the change in the value of the exponent from α_{nr} to α_r , we adopt instead the following generalization of equation (9):

$$\Gamma_s \beta_s = p(1 + p^2)^{0.12}, \quad (14)$$

$$p \equiv A \left(\frac{\tilde{E}_{\text{in}}}{\tilde{m}} \right)^{1/2} \left(\frac{\tilde{m} M_{\text{ej}}}{\rho r^3} \right)^{\alpha_{\text{nr}}}. \quad (15)$$

For the density distributions described above, our numerical results give $\alpha_{\text{nr}} = 0.187$, in agreement with the nonrelativistic self-similar theory and equation (3). We adopt this numerical value in our subsequent formulae. α_{nr}^{-1} enters in many of our expressions and we set this equal to 5.35. In the ultrarelativistic regime ($p \gg 1$), equation (14) was chosen to reproduce the approximate result $\alpha_r \simeq 0.232$ obtained by Johnson & McKee (1971).

In Figures 1 and 2 we compare equations (9) and (15) to the results of our model simulations of explosions in the “external power law” and “stellar” density distributions. The two shock velocity formulae under consideration are extremely similar, differing by only very small powers of their parameters in both the non- and ultrarelativistic limits. Their differences are most clearly seen in the stellar model, where density, and hence shock velocity, spans a greater range.

Limited numerical resolution does not allow us to follow the acceleration of a nonrelativistic shock

into the ultrarelativistic regime. Instead we have increased the explosion energy to investigate acceleration in different velocity regimes. Our results show that our improved shock propagation model (eq. [14]) is accurate to within $\pm 5\%$ for all energies and density distributions tested.³ Furthermore we find the simple Gnatyk scaling under predicts the acceleration of relativistic shocks and over-predicts the acceleration of nonrelativistic shocks. Our highest energy explosion of the stellar model shows that the Gnatyk scaling underestimates, by $\sim 33\%$, the value of Γ_s reached by a shock that accelerates from $\Gamma_s \beta_s \sim 1$ to $\Gamma_s \beta_s \sim 10$. The final Lorentz factor, Γ_f , achieved by shocked ejecta depends sensitively on Γ_s (see §2.2). For example, postshock acceleration amplifies the above decrement into a factor of three error in Γ_f .

We must note that our approximation (eqs. [14] & [15]) gives $\Gamma_s \propto (\tilde{E}_{\text{in}}/\tilde{m})^{0.56}$ rather than the correct scaling $\Gamma_s \propto (\tilde{E}_{\text{in}}/\tilde{m})^{1/2}$ that obtains in spherical, ultrarelativistic blast waves (Blandford & McKee 1976). Because of this, the accuracy of our formula breaks down for blast waves that start out ultrarelativistically; i.e. with $\tilde{E}_{\text{in}} > 1$. We begin to see these deviations by the time $\tilde{E}_{\text{in}} \sim 0.3$, as the value of A tends to increase slightly ($\lesssim 10\%$), for a given density distribution. Equations (14) and (15) are strictly valid only for trans-relativistic blast waves, i.e. for shocks that are non- or semi-relativistic to begin with, but that may accelerate to high Γ_s , i.e. $\tilde{E}_{\text{in}} \lesssim \mathcal{O}(1)$. This is well satisfied for most of the astrophysical contexts to which we shall apply the formula in §3, e.g., our model for supernova 1998bw has $\tilde{E}_{\text{in}} \simeq 0.003$. However, the extreme hypernova models considered in §3.2 are at the limits of this approximation’s validity, with $\tilde{E}_{\text{in}} \simeq 0.6$.

2.2. Postshock Acceleration

After the entire stellar envelope has been traversed by the shock wave, it is left in a state of outward motion. However, its heat content is comparable to its kinetic energy, so it will accelerate considerably as heat is converted into motion. As-

³This is after allowing for the normalization constant, A , to increase slightly with \tilde{E}_{in} for energetic explosions, e.g., for the external power law envelope model, the low energy ($\tilde{E}_{\text{in}} \leq 0.03$) explosions have $A = 0.68$ as predicted from eq. (6), while for $\tilde{E}_{\text{in}} = 0.1, 0.3$, $A = 0.72, 0.74$.

suming a strict conservation of lab-frame energy in each mass element – from the postshock state to a state of free expansion – allows one to roughly estimate the magnitude of this acceleration. However, this is a significant underestimate of the acceleration since the outermost layers gain energy at the expense of the slower ejecta within them, because of a steeply declining pressure gradient.

The relativistic strong shock jump conditions give (Blandford & McKee 1976)

$$\Gamma_s^2 = \frac{(\Gamma_2 + 1)[\hat{\gamma}(\Gamma_2 - 1) + 1]^2}{\hat{\gamma}(2 - \hat{\gamma})(\Gamma_2 - 1) + 2}, \quad (16)$$

where the subscript 2 refers to the fluid immediately behind the shock. For $\hat{\gamma} = 4/3$, we have $\beta_s/\beta_2 = 7/6$ and $\Gamma_s/\Gamma_2 = \sqrt{2}$ in the non- and ultrarelativistic limits, respectively.

Now consider the postshock acceleration of material that was struck by a nonrelativistic, strong shock as it approached the periphery of the progenitor star. Thermal and kinetic energies are in perfect equipartition behind the shock. Therefore, strict energy conservation in each element implies $\beta_f/\beta_2 = \sqrt{2}$ and so $\beta_f/\beta_s = 6\sqrt{2}/7 = 1.21$. This should be contrasted with the results of self-similar shock acceleration and postshock acceleration, which for $\hat{\gamma} = 4/3$ yield $\beta_f/\beta_s = 2.16$ and 2.04 for $n = 3/2$ and 3, respectively (Matzner & McKee 1999). Thus, the energy per baryon increases by factors of 3.2 and 2.8 in these two cases due to the concentration of energy in the fastest ejecta.

This phenomenon is even more dramatic in the context of relativistic acceleration, where the postshock energy density is dominated by internal energy rather than the rest mass of the fluid. For a strong relativistic shock, the total postshock energy per unit rest mass, evaluated in the fixed frame and neglecting terms of order Γ_s^{-2} , is $4\Gamma_2^2/3 = 2\Gamma_s^2/3$ (Blandford & McKee 1976). If each baryon maintained exactly this share of energy into the final state of cold, free expansion, then $2\Gamma_s^2/3$ would also equal its terminal Lorentz factor Γ_f . The theory of acceleration behind an ultrarelativistic shock was treated approximately by Johnson & McKee (1971), who estimated $\Gamma_f \simeq (\Gamma_s/\sqrt{2})^{1+\sqrt{3}}$ as a lower limit.⁴ In this case, postshock acceleration increases the

energy per particle by a factor of approximately $\Gamma_s^{0.73}$. As this is a large factor, the postshock acceleration, and the concentration of energy in the fastest material, are even more impressive in the relativistic case.

These considerations demonstrate that the acceleration of the fluid after it is shocked is critical to the distribution of energy with Lorentz factor in the ejecta. The character of planar postshock acceleration is qualitatively different in the non-relativistic case, where the velocity increases by a fixed factor, from the relativistic case, where the final Lorentz factor becomes a power of the postshock value. However, in both cases there is a functional relationship between $\Gamma_f\beta_f$ and $\Gamma_s\beta_s$. In reality there is a dependence on the slope of the density distribution as well, but this is quite weak and we are justified in ignoring it. Hence our goal is to find an approximate analytical relationship between the final velocity of a fluid element and the velocity of the shock that struck it: one that obeys the known limits and remains sufficiently accurate in the trans-relativistic regime. We shall begin by examining postshock acceleration in strictly planar geometry. Then we shall consider how spherical expansion may reduce the terminal Lorentz factor of the ejecta relative to the planar case.

2.2.1. Planar Geometry

We continue with the density distribution $\rho = \rho_h(1 - r/R)^n \equiv \rho_h x^n$, with $n = 3$, which now describes a planar slab of material of length R . We release shocks of varying strengths that propagate down this density ramp. In regions significantly far away from the launching region ($R - r \ll R$), and except for the effects of finite resolution, the shock and postshock behavior ought to be the same among all of these runs – i.e., the function $\Gamma_f\beta_f(\Gamma_s\beta_s)$ should have the same form. This follows from the fact that a power law density distribution introduces no scales of its own. By exploring the relation between shock and postshock velocities in simulations of different initial shock strength, we are able to discriminate this common behavior from the artifacts of the particular initial conditions or of the finite numerical resolution: see

multiplicative constant if the rest mass of the fluid were included in the equation of state.

⁴Johnson & McKee (1971) showed Γ_f would increase by a

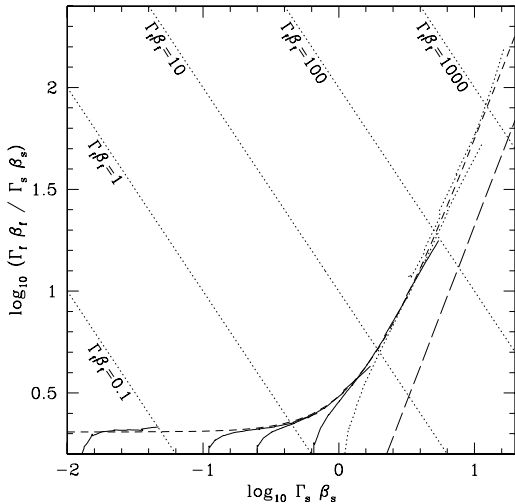


Fig. 3.— Final fluid velocity ($\Gamma_f \beta_f$) in the *planar* free coasting state compared to the velocity of the shock ($\Gamma_s \beta_s$) striking a particular fluid element, as a function of $\Gamma_s \beta_s$. Numerical results for different initial energies are shown by the heavy *solid* and *dotted* lines. The *dotted* lines, at the highest energies, have the greatest systematic uncertainties from corrections for incomplete convergence. The *dashed* line is our expression for planar post-shock acceleration $\Gamma_f \beta_f / \Gamma_s \beta_s = C_{\text{nr}} + (\Gamma_s \beta_s)^{\sqrt{3}}$ (eq. [17]). The inclined *long dashed* line is the ultrarelativistic prediction of Johnson & McKee (1971), $\Gamma_f = \Gamma_2^{1+\sqrt{3}} = 0.39 \Gamma_s^{1+\sqrt{3}}$, which we find underestimates Γ_f by a factor of ~ 2.6 .

Figure 3.

For the purposes of numerical stability, we allow the fluid to expand into a uniform medium of sufficiently low density that its effects on the accelerating ejecta (a reverse shock) can be visualized and excluded from consideration. Because the conversion of internal into kinetic energy is quite slow in planar expansion, and because of time-step constraints on our code, it was necessary to examine the approach of mass elements toward their terminal velocities in order to estimate how much acceleration would occur if they were allowed to expand indefinitely. A correction to $\Gamma\beta$ based on the extrapolation of internal energy to zero was made. Typical values of this correction were $\lesssim 5 - 10\%$ for the lower energy runs (*solid* lines in Figure 3). For the most relativistic cases considered (*dotted* lines) the correction was $\sim 20 - 30\%$. This correction procedure was checked and validated against the end state of a single simulation, allowed to expand out to a very large distance, at which point the internal energy of the zones was negligible. These corrected results were then further corrected for incomplete numerical convergence, for both the shock and final velocities, by considering the results as a function of the number of simulation zones. The largest values of these corrections, again for the most relativistic runs, were $\sim 50\%$.

We find that the following analytical formula captures the relationship between shock and terminal velocities:

$$\frac{\Gamma_f \beta_f}{\Gamma_s \beta_s} \simeq C_{\text{nr}} + (\Gamma_s \beta_s)^{\sqrt{3}}. \quad (17)$$

For density distributions with $n \simeq 3$, $C_{\text{nr}} = 2.03$ (Matzner & McKee 1999). Comparing to numerical simulations, equation (17) is accurate to $\pm 10\%$ for $\Gamma_s \beta_s \lesssim 5$, corresponding to $\Gamma_f \beta_f \lesssim 100$; and $\pm 25\%$ for $\Gamma_s \beta_s \lesssim 10$, corresponding to $\Gamma_f \beta_f \lesssim 500$. The uncertainty is greatest for the most relativistic ejecta. In the ultrarelativistic limit, equation (17) tends towards the scaling predicted by Johnson & McKee (1971), but increased by a factor of $\sqrt{2}^{1+\sqrt{3}} \simeq 2.6$.

2.2.2. Spherical geometry

The above calculation assumes that planar symmetry holds throughout the postshock acceleration phase of the ejecta. In fact, the planar,

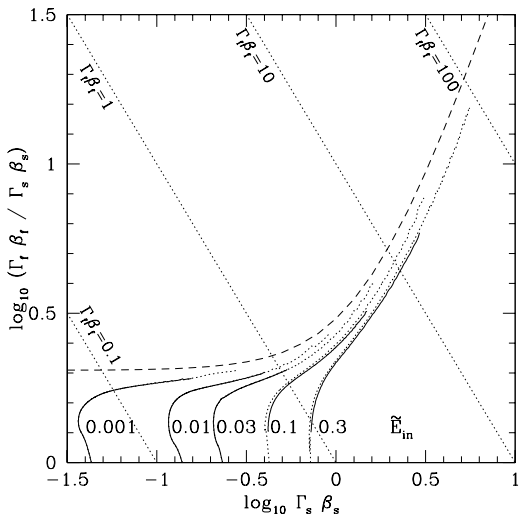


Fig. 4.— Spherical postshock acceleration for simulations with $\tilde{E}_{\text{in}} = 0.001, 0.01, 0.03, 0.1, 0.3$. *Solid* lines are regions where we have corrected for numerical convergence. *Dotted* lines are the highest resolution results without such a convergence correction. The *dashed* line shows the planar result from Figure 3.

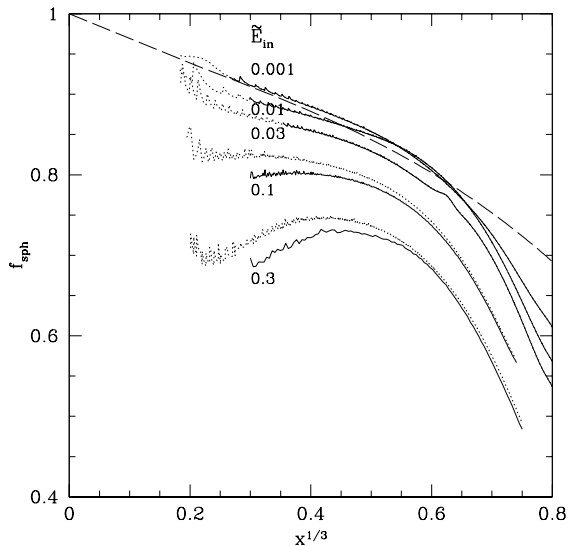


Fig. 5.— Deviation of spherical postshock acceleration from the planar limit (equation 17) as a function of $x^{1/3} \equiv (1 - r/R)^{1/3}$, for simulations with a power-law initial density distribution ($\rho \propto x^3$) and $\tilde{E}_{\text{in}} = 0.001, 0.01, 0.03, 0.1, 0.3$. The *solid* and *dotted* lines are the same as in Figure 4. The *long dashed* line shows the nonrelativistic prediction for f_{sph} for an $n = 3$ polytrope (eq. [19]). For $x^{1/3} > 0.6$ the chosen initial conditions no longer approximate a polytrope, which explains the discrepancy between theory and simulation in this region for nonrelativistic ejecta. Uncertainties in the planar solution also contribute to the accuracy of this prediction.

nonrelativistic flow approaches its terminal velocity extremely slowly: any fluid element must travel many times its initial depth before acceleration is complete. Once the fluid has traveled a distance of order the stellar radius, however, its volume is significantly larger than in the planar approximation, and its pressure is correspondingly less. This causes nonrelativistic acceleration to cease at some radius, as originally suggested by Litvinova & Nadézhin (1990). Comparing to nonrelativistic numerical simulations, Matzner & McKee (1999) find that the results of spherical expansion match the results of planar acceleration, truncated at three stellar radii; this is also consistent with the analytical theory of Kazhdan & Murzina (1992). In terms of the normalized depth $x \equiv 1 - r/R$, Matzner & McKee (1999) find that spherical truncation reduces the terminal velocity of a mass element originally at depth xR by the factor

$$f_{\text{sph,nr}}(n = 1.5) = 1 - 0.51x^{1/3} + 0.76x^{2/3} - 1.19x \quad (18)$$

$$f_{\text{sph,nr}}(n = 3) = 1 - 0.34x^{1/3} + 0.24x^{2/3} - 0.37x \quad (19)$$

for polytropes of these indices. These results on postshock acceleration are valid for polytropic envelopes in an outer region with $\tilde{m}_{\text{ex}} \equiv 1 - \tilde{m} \ll 1$, and $x^{1/3} \lesssim 0.8$. Deeper into the envelope, polytropes differ in structure if they enclose different core masses; this, along with changing dynamics deep within the explosion, causes deviations from these common forms (Matzner & McKee 1999).

We have followed the postshock acceleration of ejecta from spherical explosions of different energies, using for a progenitor the external power law distribution $\rho = \rho_h(1 - r/R)^3 \equiv \rho_h x^3$, to examine how spherical truncation, expressed via

$$f_{\text{sph}} \equiv \frac{(\Gamma_f \beta_f)_{\text{spherical}}}{(\Gamma_f \beta_f)_{\text{planar}}}, \quad (20)$$

changes as velocities become more and more relativistic. Figures 4 and 5 compare the planar law (eq. [17]) with spherical numerical results. The predicted nonrelativistic truncation (eq. [19]) is recovered for $x^{1/3} < 0.6$, where $\rho \propto x^3$ well approximates a polytrope. At higher energies and velocities we observe more significant truncation in the outermost ejecta. $\Gamma_f \beta_f$ is reduced to $\sim 70\%$ of the predicted planar value in the most relativistic

case. We note this estimate is somewhat uncertain, because of uncertainties in the planar solution to which we make comparison.

For purposes of estimating the final energy distribution of the outer ($x < 0.3$, $x^{1/3} < 0.67$) ejecta we approximate f_{sph} as a constant factor, independent of x , varying between 0.85 and 0.7 as \tilde{E}_{in} is increased from 0.0 to 0.3. This behavior is captured by

$$f_{\text{sph}} = 0.85 - \tilde{E}_{\text{in}}^{1/2}/4, \quad (21)$$

which is approximately the value of f_{sph} at $x = 0.125$. This expression is accurate to $\pm 15\%$ at any given x , tending to underestimate velocities at $x < 0.125$, and overestimate those at $x > 0.125$. It has greater accuracy for predicting the mean value of f_{sph} for $0.0 < x < 0.3$.

Combining expressions (14), (17), and (21), the final velocity of a mass element is

$$\begin{aligned} \Gamma_f \beta_f &= (0.85 - \tilde{E}_{\text{in}}^{1/2}/4)p(1 + p^2)^{0.12} \\ &\quad \times [2.03 + p^{1.73}(1 + p^2)^{0.21}] \\ &\simeq (0.85 - \tilde{E}_{\text{in}}^{1/2}/4)(1.80p^{5/6} + p^{2.82})^{6/5}, \end{aligned} \quad (22)$$

where the second line approximates the first within 1.5%. Either approximation holds within 15% only in the outermost $\sim 30\%$ of the stellar radius, where equation (21) is valid.

In an outer layer ($x \lesssim 0.2$), the polytropic distribution (eq. [10]) limits to the power-law form (eq. [12]). The mass and density are then related by (Matzner & McKee 1999)

$$\rho = f_\rho \frac{M_{\text{ej}}}{R^3} \tilde{m}_{\text{ex}}^{1/\gamma_p}, \quad (x \ll 1), \quad (23)$$

where

$$\gamma_p \equiv 1 + 1/n, \quad (24)$$

$$f_\rho = \left(\frac{n+1}{4\pi} \right)^{1/\gamma_p} \tilde{\rho}_h^{1/(n+1)}, \quad (25)$$

which is Matzner & McKee's $f_{\rho_0}(1)$, and we have defined

$$\tilde{\rho}_h \equiv \frac{\rho_h R^3}{M_{\text{ej}}}, \quad (26)$$

which is Matzner & McKee's parameter ρ_1/ρ_* . For $n \simeq 3$, equation (23) is valid to within 10% for $r > 0.96R$ and to within 50% for $r > 0.75R$. The scaling $\rho^{\gamma_p} \propto \tilde{m}_{\text{ex}}$ arises from the hydrostatic relation between mass and pressure in a thin sub-surface layer.

In this outer power-law region, p can be evaluated by approximating $r \simeq R$ and $\tilde{m} \simeq 1$ in equation (15):

$$p \simeq A \tilde{E}_{\text{in}}^{1/2} \left(\frac{\rho R^3}{M_{\text{ej}}} \right)^{-0.187} \quad (27a)$$

$$\simeq A \tilde{E}_{\text{in}}^{1/2} \tilde{\rho}_h^{-0.187} x^{-0.187n} \quad (27b)$$

$$\simeq A \tilde{E}_{\text{in}}^{1/2} f_\rho^{-0.187} \tilde{m}_{\text{ex}}^{-0.187/\gamma_p}, \quad (27c)$$

where equations (27b) and (27c) use (12) and (23), respectively. The error introduced by adopting these power law approximations for p is roughly x , and in the outer fifth of the radius it is smaller than the error introduced by f_{sph} in equation (21).

As we have noted, equation (21) for the parameter f_{sph} , and the power law representations for p in equation (27), break down for $x \gtrsim 0.25$. As the shock intensity p increases outward near the surface of the star, this implies that there exists a minimum value of p (hence, from eq. [22], a minimum final velocity) for which our equations accurately predict the final velocity. To estimate this criterion, we may set $x \lesssim 0.25$ and estimate $A \simeq 0.736$ in equation (27b) to find

$$p \gtrsim 0.736 \exp(0.26n) \tilde{E}_{\text{in}}^{1/2} \tilde{\rho}_h^{-0.187}. \quad (28)$$

2.3. Kinetic Energy Distribution of the Ejecta

In order to estimate the observable properties of relativistic mass ejection from astrophysical explosions, it will be useful to know the kinetic energy in ejecta above some velocity $E_k(> \Gamma_f \beta_f)$. This information is available through the formulae presented in §§2.1 and 2.2. In this section, we shall use the above results to present more convenient analytical formulae for $E_k(> \Gamma_f \beta_f)$. We restrict our attention to a shell of material from the outermost layers of the star, whose mass is negligible ($\tilde{m}_{\text{ex}} \equiv 1 - \tilde{m} \ll 1$) and through which the shock accelerated. We approximate the spherical truncation with eq. (21), which tends to underestimate the kinetic energy in relativistic ejecta, and overestimate the energy in nonrelativistic ejecta, although never by more than 15%.

The fraction of the rest mass energy transmitted into kinetic energy at velocities above $\Gamma_f \beta_f$

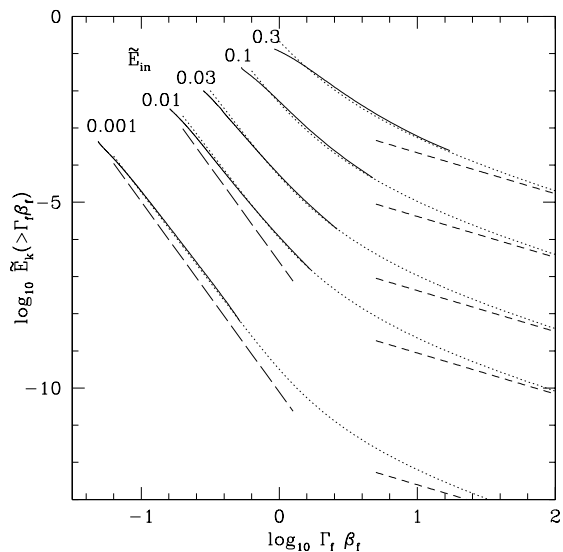


Fig. 6.— Cumulative kinetic energy distribution of ejecta from a progenitor with $\rho = \rho_h(1 - r/R)^3$ for $\tilde{E}_{\text{in}} = 0.001, 0.01, 0.03, 0.1, 0.3$. *Solid* lines - converged results from numerical simulation; *dotted* lines - analytic estimate (eq. 37); *dashed* lines - relativistic limit (eq. 36); and *long-dashed* lines - nonrelativistic limit (equation 35) shown for the two lowest energy cases.

is

$$\tilde{E}_k(> \Gamma_f \beta_f) = \int_0^{\tilde{m}_{\text{ex}}} (\Gamma_f - 1) d\tilde{m}'_{\text{ex}}, \quad (29)$$

where \tilde{m}_{ex} refers to the ejecta traveling faster than $\Gamma_f \beta_f$.

Lacking a relativistic theory, Matzner & McKee (1999) estimated the energy in relativistic ejecta as $M_{\text{rel}} c^2$, where M_{rel} is the mass in which an extrapolation of the nonrelativistic expressions (ignoring spherical truncation) predicts $\beta_f > 1$. Examining equations (3), (15) and (17), we find that this definition corresponds to $p > 1/C_{\text{nr}}$:

$$M_{\text{rel}} \equiv \tilde{m}_{\text{ex}}(p > 1/C_{\text{nr}}) M_{\text{ej}}. \quad (30)$$

Equations (14) and (17), together with allowance for spherical truncation (eq. [20]), show that the ejecta with mass M_{rel} expand with $\Gamma_f \beta_f > 1.18 f_{\text{sph}}$; if $f_{\text{sph}} \simeq 0.85$, as indicated by equation (21), this is $\Gamma_f \beta_f > 1.00$. M_{rel} is thus an excellent estimate of the mass in relativistic ejecta.

For a stellar progenitor with a polytropic atmosphere, Matzner & McKee (1999) find

$$\begin{aligned} M_{\text{rel}} &\simeq 10^{28.5-4.8/n} f_{\rho}^{-\gamma_p} \left(\frac{A}{0.794} \right)^{5.35\gamma_p} \\ &\times \left(\frac{E_{\text{in}}}{10^{52} \text{ erg}} \right)^{2.67\gamma_p} \left(\frac{M_{\text{ej}}}{1 M_{\odot}} \right)^{1-2.67\gamma_p} \text{ g}, \end{aligned} \quad (31)$$

where f_{ρ} is defined in equation (23) and we have included the dependence on A ; we shall present equivalent expressions for progenitors with radiative outer envelopes below.

Equation (31) assumes that the shock velocity is a power law in depth. This assumption is valid in the outer $\sim 25\%$ of the stellar radius; equivalently, it holds when the value $p = 1/C_{\text{nr}} = 0.49$, which corresponds to M_{rel} , is above the lower limit in equation (28). This requires

$$\tilde{E}_{\text{in}} \lesssim 0.44 \exp(-0.52n) \tilde{\rho}_h^{0.374}. \quad (32)$$

If this condition is not satisfied, the value of M_{rel} in equation (31) will under predict the mass in material with $p > 0.49$, and equation (21) will over predict its final velocity. Even so, M_{rel} remains an accurate coefficient for higher-velocity ejecta that do arise in the outer quarter of the radius; c.f. equations (41) and (42) below.

To evaluate $M_{\text{rel}} c^2$ as an estimate of the kinetic energy in relativistic ejecta, and to determine the distribution of kinetic energy with velocity, we must evaluate equation (29). For nonrelativistic ejecta, equations (14), (15), (17), and (23) give $\beta_f \propto \tilde{m}_{\text{ex}}^{-\alpha_{\text{nr}}/\gamma_p} \propto \tilde{m}_{\text{ex}}^{-0.187/\gamma_p}$, for $r \simeq R$ and $\tilde{m} \simeq 1$. Since $\tilde{E}_k(> \Gamma_f \beta_f) = \int_0^{\tilde{m}_{\text{ex}}} \beta_f^2 d\tilde{m}'_{\text{ex}}/2$ for nonrelativistic ejecta, this implies that

$$\tilde{E}_k(> \Gamma_f \beta_f) = \frac{\beta_f^2 \tilde{m}_{\text{ex}}}{2 - 0.75/\gamma_p}. \quad (33)$$

For extremely relativistic ejecta, the same equations give $\Gamma_f \propto \tilde{m}_{\text{ex}}^{-0.634/\gamma_p}$, and since $\tilde{E}_k(> \Gamma_f \beta_f) = \int_0^{\tilde{m}_{\text{ex}}} \Gamma_f d\tilde{m}'_{\text{ex}}$ in this limit,

$$\tilde{E}_k(> \Gamma_f \beta_f) = \frac{\Gamma_f \tilde{m}_{\text{ex}}}{1 - 0.63/\gamma_p}. \quad (34)$$

Note that the energy above some final velocity $\Gamma_f \beta_f$ is proportional to the mass \tilde{m}_{ex} in ejecta above that velocity, quite generally. This follows from equations (17) and (21), which demonstrate that the final velocity is essentially a universal function of the shock velocity for a given element, modulo slight variations in f_{sph} not captured in equation (21). Therefore, $\tilde{E}_k(> \Gamma_f \beta_f)$ is proportional to mass of ejecta that was hit by a shock going faster than the corresponding shock velocity $\Gamma_s \beta_s$.

Eliminating \tilde{m}_{ex} from equations (33) and (34) by means of equations (14), (17), (20) and (23), we find in the non- and ultrarelativistic limits

$$\begin{aligned} \tilde{E}_k(> \Gamma_f \beta_f) &\simeq \frac{(f_{\text{sph}} C_{\text{nr}} A \tilde{E}_{\text{in}}^{1/2})^{5.35\gamma_p}}{2 - 0.75/\gamma_p} \\ &\times f_{\rho}^{-\gamma_p} (\Gamma_f \beta_f)^{-(5.35\gamma_p-2)} \\ &[\Gamma_f \beta_f \ll 1] \end{aligned} \quad (35)$$

and

$$\begin{aligned} \tilde{E}_k(> \Gamma_f \beta_f) &\simeq \frac{(f_{\text{sph}}^{0.295} A \tilde{E}_{\text{in}}^{1/2})^{5.35\gamma_p}}{1 - 0.63/\gamma_p} \\ &\times f_{\rho}^{-\gamma_p} (\Gamma_f \beta_f)^{-(1.58\gamma_p-1)} \\ &[\Gamma_f \beta_f \gg 1] \end{aligned} \quad (36)$$

respectively. One formula that attains each of these limits is

$$\tilde{E}_k(> \Gamma_f \beta_f) = (A \tilde{E}_{\text{in}}^{1/2})^{5.35\gamma_p} f_{\rho}^{-\gamma_p} F(\Gamma_f \beta_f), \quad (37)$$

where

$$\begin{aligned}
F(\Gamma_f \beta_f) &\equiv \frac{(f_{\text{sph}}^{1-0.705\beta_f} C_{\text{nr}}^{1-\beta_f})^{5.35\gamma_p}}{2 - \beta_f - (0.75 - 0.11\beta_f)/\gamma_p} \\
&\times \left[(\Gamma_f \beta_f)^{-(5.35-2/\gamma_p)/q} \right. \\
&\quad \left. + (\Gamma_f \beta_f)^{-(1.58-1/\gamma_p)/q} \right]^{q\gamma_p}. \quad (38)
\end{aligned}$$

We find that setting $q = 4.1$ gives an excellent fit to the simulation results, as Figure 6 demonstrates. This fit is more precise than deriving $E_k(> \Gamma_f \beta_f)$ from equations (27c), (14), (17), and (21), principally because details of the spherical truncation are not captured in equation (21). Note that for progenitor density distributions that fall off rapidly near their edges, the energy contained in ejecta above a particular velocity is quite sensitive to the degree of shock and postshock acceleration. For example a 10% error in the final velocity caused by equation (21) can lead to a factor of two error in $\tilde{E}_k(> \Gamma_f \beta_f)$ in the nonrelativistic limit. Variations in the polytropic index n may cause α_{nr} to vary by a few percent (Sakurai 1960). Such differences may be amplified into large variations in $\tilde{E}_k(> \Gamma_f \beta_f)$, typically $\sim 50\%$. Note that the ultrarelativistic limit is approached only very slowly, i.e. for $\Gamma_f \beta_f \gtrsim 100$. This is because the Lorentz factor of the shock, Γ_s , needs to be relativistic for these limits to apply and $\Gamma_f \beta_f \gg \Gamma_s \beta_s$ in the relativistic regime (eq. 17). Figure 6 also illustrates that the cumulative energy distribution deviates from equation (37) in the lowest-velocity ejecta. This is due to the failure of several of our assumptions in this material: r is no longer close to R , f_{sph} decreases at lower velocities, and the dynamics changes once $\tilde{m}_{\text{ex}} \ll 1$ is no longer valid; these issues were treated in detail by Matzner & McKee (1999).

Expression (37) is a remarkably simple estimate of the fast and relativistic ejecta from a stellar explosion. In the following sections, we shall use it to predict the outcomes of explosions within radiative stellar envelopes, and of asymmetrical explosions. We wish therefore to re-express (37) in a couple of forms that will facilitate these investigations.

First, suppose one knows that the shock exceeds an intensity p' in a small fraction $\tilde{m}_{\text{ex}}(> p')$ of the total ejecta. What will be the kinetic energy in ejecta faster than $\Gamma_f \beta_f$, where $\Gamma_f \beta_f$ is arbitrary?

Using equations (14), (15), and (23), we rewrite (37) as

$$\tilde{E}_k(> \Gamma_f \beta_f) \simeq p'^{5.35\gamma_p} \tilde{m}_{\text{ex}}(> p') F(\Gamma_f \beta_f). \quad (39)$$

Here, the combination $p'^{5.35\gamma_p} \tilde{m}_{\text{ex}}(> p')$ is a constant independent of p' , so long as it is evaluated in the outermost $\sim 25\%$ of the radius (e.g., as in eq. 27c). This leads equations (35), (36), and (37) to obey the scaling (in dimensional variables)

$$E_k(> \Gamma_f \beta_f) \propto [E_{\text{in}}/(M_{\text{ej}}c^2)]^{2.67\gamma_p} M_{\text{ej}}c^2. \quad (40)$$

Second, we may express $E_k(> \Gamma_f \beta_f)$ in terms of the rest mass scale M_{rel} for relativistic ejecta. Taking $f_{\text{sph}} = 0.85$ and $p' = 1/C_{\text{nr}} = 0.49$, equation (39) gives

$$E_k(> \Gamma_f \beta_f) \simeq \frac{F(\Gamma_f \beta_f)}{C_{\text{nr}}^{5.35\gamma_p}} M_{\text{rel}}c^2. \quad (41)$$

Evaluating this at the transition from nonrelativistic to relativistic motion ($\Gamma_f \beta_f = 1$),

$$E_k(> 1) \simeq 1.23 \frac{n+1}{n+2.1} \exp\left(-\frac{1}{3.7n}\right) \left(\frac{f_{\text{sph}}}{0.85}\right)^{2.67\gamma_p} M_{\text{rel}}c^2. \quad (42)$$

Hence $E_k(> 1) \simeq (0.71, 0.88, 0.94, 1.07) M_{\text{rel}}c^2$ for $n = (1.5, 3, 4, 9)$, respectively, justifying $M_{\text{rel}}c^2$ as an energy scale for relativistic motion.

2.4. Envelope Structure and the Efficiency of Fast Ejecta Production

An accelerating shock front produces rapid ejecta in much the same manner as a whip produces its crack: by concentrating a diminishing fraction of its energy in an even more rapidly diminishing fraction of the total mass, as a disturbance travels outward. On Earth, whips are fashioned to yield the sharpest report for the least effort, so we may ask: What qualities in a stellar progenitor will maximize the energy in ejecta above a given velocity?

To address this question, we rewrite equation (27c) with $p = 0.49$, as

$$\frac{M_{\text{rel}}}{M_{\text{ej}}} = \left[\left(\frac{A}{0.736} \right)^2 \frac{2.23\tilde{E}_{\text{in}}}{f_p^{0.374}} \right]^{2.67\gamma_p}. \quad (43)$$

This ratio represents the efficiency with which a given explosion creates relativistic ejecta. For a

given value of \tilde{E}_{in} , what properties of the ejected envelope enhance $M_{\text{rel}}/M_{\text{ej}}$? Note that $A/0.736$ and f_ρ are both roughly unity; moreover, equation (27c) is validated only for $\tilde{E}_{\text{in}} \lesssim 0.3$. For the mildly relativistic explosions to which (43) applies, it states that $M_{\text{rel}}/M_{\text{ej}}$ is a small number raised to the power $2.67\gamma_p$. The relativistic yield of an explosion is therefore enhanced by making γ_p as small as possible, i.e., by making n as large as possible. For a fixed value of γ_p , the relativistic yield is also enhanced by decreasing f_ρ , or equivalently, by decreasing the outer density coefficient $\tilde{\rho}_h$. Both of these results can be interpreted to say that more centrally concentrated envelopes are more efficient at producing relativistic ejecta.

Second, note that the relativistic ejecta of a trans-relativistic explosion are enhanced – both in absolute terms and as a fraction of the total – if E_{in} is increased or M_{ej} is reduced. For a given progenitor mass, the relativistic yield is thus enhanced by allowing as much of the star as possible to collapse.

Equations (41) and (42) demonstrate that the kinetic energy at *any* final velocity $\Gamma_f\beta_f$ (relativistic or otherwise) is proportional to $M_{\text{rel}}c^2$, so long as this ejecta originated from a thin outer layer in which the shock accelerated; therefore, the above conclusions apply to fast ejecta even when the maximum ejecta velocity is nonrelativistic.

Let us examine the criterion for relativistic ejecta to exist. The alternative is that the shock diffuses through the surface before p reaches 0.49, the value for which $\Gamma_f\beta_f > 1$. The optical depth of a nonrelativistic shock front is $\tau_s \sim 1/p$ (Weaver 1976), whereas the optical depth of the layer with mass M_{rel} is $\tau = \kappa M_{\text{rel}}/(4\pi R^2)$, where κ is the opacity. To contain the shock front when $p = 0.49$, $\tau > \tau_s \simeq 2$, or

$$R \lesssim 55 \left(\frac{\kappa}{0.34 \text{ cm}^2 \text{ g}^{-1}} \frac{M_{\text{rel}}c^2}{10^{48} \text{ erg}} \right)^{1/2} R_\odot. \quad (44)$$

This constraint on R , which is easily satisfied by the model CO6 considered below ($M_{\text{rel}}c^2 \sim 10^{48}$ erg; $R \sim R_\odot/6$), becomes less restrictive as M_{rel} increases.

The mass M_{rel} in relativistic ejecta, and the corresponding kinetic energy $E_k(> 1)$, can be derived from equation (43) using the equilibrium structures of stars with radiative outer envelopes. In

the case of a constant (e.g., electron scattering) opacity, $n = 3$ and

$$f_\rho = 0.148 \left(\frac{M_\star}{M_{\text{ej}}} \right)^{1/4} \frac{1 - L_\star/L_{\text{edd}}}{(L_\star/L_{\text{edd}})^{1/4}} \left(\frac{\mu}{0.62} \right) \left(\frac{M_\star}{10 M_\odot} \right)^{1/2} \quad (45)$$

(Matzner & McKee 1999; note typo in their eq. 12), where μ is the mean molecular weight in amu and L_{edd} is the Eddington limiting luminosity. Using (43) and (45), we find that the fraction of the ejected mass that becomes relativistic is

$$\frac{M_{\text{rel}}}{M_{\text{ej}}} = 430\mu^{-4/3} \left(\frac{E_{\text{in}}}{M_{\text{ej}}c^2} \right)^{3.57} \left(\frac{A}{0.736} \right)^{7.13} \times \frac{M_{\text{ej}}^{1/3} M_{\text{Ch}}^{2/3}}{M_\star} \frac{(L_\star/L_{\text{edd}})^{1/3}}{(1 - L_\star/L_{\text{edd}})^{4/3}}, \quad (46)$$

where $M_{\text{Ch}} = 1.434 M_\odot$ is the Chandrasekhar limiting mass for an object with $\mu_e = 2$. As L_\star increases relative to L_{edd} , the outer envelope becomes significantly more dilute compared to the core; as we argued in the previous section, the efficiency of relativistic ejection, $M_{\text{rel}}/M_{\text{ej}}$, increases correspondingly. This effect can be achieved, for instance, by increasing the radiative opacity (hence lowering L_{edd}): intuitively, the envelope must expand to carry a constant flux despite the higher opacity.

Equations (42) and (46) then give

$$\begin{aligned} E_k(> 1) &= 0.88 M_{\text{rel}}c^2 \\ &\simeq (1.8, 2.6, 8.9) \times 10^{46} E_{52}^{3.57} L_5^{1/3} \\ &\times \left(\frac{M_\star}{6 M_\odot} \right)^{-4/3} \left(1 - \frac{L_\star}{L_{\text{edd}}} \right)^{-4/3} \\ &\times \left(\frac{A}{0.736} \right)^{7.13} \left(\frac{M_{\text{ej}}}{4 M_\odot} \right)^{-2.23} \text{ erg}, \quad (47) \end{aligned}$$

using $f_{\text{sph}} \simeq 0.85$, for stars with CO envelopes, He envelopes, and H envelopes of solar composition, respectively. In this equation, $L_\star \equiv 10^5 L_5 L_\odot$ and $E_{\text{in}} \equiv 10^{52} E_{52}$ erg.

If the opacity in the outer envelope (the region containing M_{rel}) is dominated instead by bound-free or free-free transitions, then M_{rel} will exceed the prediction of equation (47). Provided radiation pressure is negligible, which requires $L_\star \ll L_{\text{edd}}$, the envelope will be a polytrope with $n = 3.25$ and

$$f_\rho^{17} = \frac{2}{R} \left(\frac{\pi^2 ac}{51\kappa_0 L_\star M_{\text{ej}}^2} \right)^2 \left(\frac{GM_\star \mu M_p}{2\pi k_B} \right)^{15}. \quad (48)$$

Here $\kappa = \kappa_0 \rho T^{-3.5}$ is Kramers' opacity law; we estimate $\kappa_0 \simeq (37, 0.69, 1.24) \times 10^{24} \text{ cm}^5 \text{ g}^{-2}$ in (CO, He, H) envelopes (Harpaz 1994; Clayton 1983), by taking both relevant Gaunt factors to be ~ 0.85 (M_{rel} depends only weakly on this choice.) The energy above $\Gamma_f \beta_f = 1$ is, using $f_{\text{sph}} = 0.85$,

$$\begin{aligned} E_k(> 1) &= 0.90 M_{\text{rel}} c^2 \\ &\simeq (3.2, 2.4, 6.3) \times 10^{46} E_{52}^{3.50} L_5^{2/13} \\ &\times R_{10}^{1/13} \left(\frac{M_\star}{6 M_\odot} \right)^{-15/13} \left(\frac{A}{0.736} \right)^{6.99} \\ &\times \left(\frac{M_{\text{ej}}}{4 M_\odot} \right)^{-2.19} \text{ erg}, \end{aligned} \quad (49)$$

for (CO, He, H) envelopes, respectively, where $R \equiv 10^{10} R_{10} \text{ cm}$. In the Kramers layer, radiation pressure increases outward as a fraction of the total; when it is no longer negligible, n increases toward seven (Chandrasekhar 1939); therefore, equation (49) is an underestimate in stars with appreciable L_\star/L_{edd} . In general, the larger of (47) and (49) gives a lower limit for the kinetic energy of relativistic material.

Let us examine the criteria for equations (47) and (49) to correctly represent the energy in relativistic ejecta. The first of these is given by condition (32), which states that M_{rel} must originate from the outer quarter of the radius, to correctly give $E_k(> 1)$. For (CO, He, H) electron-scattering atmospheres this becomes, using eq. (45),

$$\begin{aligned} \tilde{E}_{\text{in}} &\lesssim (0.12, 0.081, 0.021) \left(\frac{0.736}{A} \right)^2 \\ &\times \left[\left(1 - \frac{L_\star}{L_{\text{edd}}} \right)^4 L_5^{-1} \left(\frac{M_\star}{6 M_\odot} \right)^4 \frac{4 M_\odot}{M_{\text{ej}}} \right]^{0.374} \end{aligned} \quad (50)$$

Using eq. (48) to express the same condition for Kramers atmospheres with negligible radiation pressure,

$$\begin{aligned} \tilde{E}_{\text{in}} &\lesssim (0.087, 0.15, 0.037) \left(\frac{0.736}{A} \right)^2 \\ &\times \left[L_5^{-1} R_{10}^{-1/2} \left(\frac{M_\star}{6 M_\odot} \right)^{15/2} \left(\frac{4 M_\odot}{M_{\text{ej}}} \right)^2 \right]^{0.187} \end{aligned} \quad (51)$$

in the same three cases. However, recall that M_{rel} can be used to predict the distribution of ejecta at sufficiently relativistic velocities (eqs. [41] and

[42]), even when this condition indicates that it does not accurately determine $E_k(> 1)$.

In contrast, there are no relativistic ejecta at all if the shock breaks out of the star before $p > 0.49$. This condition, expressed above in equation (44), gives for Thomson atmospheres

$$\begin{aligned} R_{10} &\lesssim (43, 51, 122) \left(\frac{A}{0.736} \right)^{3.57} L_5^{1/6} E_{52}^{1.78} \\ &\times \left(1 - \frac{L_\star}{L_{\text{edd}}} \right)^{-2/3} \left(\frac{6 M_\odot}{M_\star} \right)^{2/3} \left(\frac{4 M_\odot}{M_{\text{ej}}} \right)^{1.12} \end{aligned} \quad (52)$$

for (CO, He, H) envelopes. In the case that Kramers opacity determines the structure of the envelope, it is still electron-scattering opacity that controls the width of the shock. Therefore, equations (44) and (48) give

$$\begin{aligned} R_{10} &\lesssim (55, 48, 101) \left(\frac{A}{0.736} \right)^{3.64} \\ &\times L_5^{2/25} E_{52}^{1.82} \left(\frac{6 M_\odot}{M_\star} \right)^{3/5} \left(\frac{4 M_\odot}{M_{\text{ej}}} \right)^{1.14} \end{aligned} \quad (53)$$

2.5. Aspherical Explosions

In equation (40), we have shown that the energy above some velocity scales as $E_{\text{in}}^{2.67\gamma_p} M_{\text{ej}}^{1-2.67\gamma_p}$. Although our results so far have been limited to spherical or planar symmetry, this scaling suggests that asymmetries in the initial explosion may be exaggerated in the angular distribution of relativistic ejecta. The dynamics of non-spherical explosions are more appropriately addressed using multidimensional numerical simulations (e.g., Chevalier & Soker 1989; MacFadyen & Woosley 1999; Höflich et al. 1999; Aloy et al. 2000). Because such simulations cannot afford the fine surface zoning necessary to capture the dynamics of shock acceleration, we wish to answer the following questions: Under what conditions may the theory developed here for spherical explosions be applied to aspherical explosions? What is the appropriate correspondence between our formulae and the outcome of an aspherical explosion?

To address the first question, it suffices to note that, during the terminal acceleration of a nonrelativistic shock and the subsequent postshock expansion (Sakurai 1960; Matzner & McKee 1999), perturbations in the postshock flow can only propagate laterally a limited distance: if the shock has

reached a depth x , then an acoustic wave launched from some point on the shock surface can only affect a region within a few times x to either side. We arrive at this conclusion by examining the self-similar solution presented by Matzner & McKee (1999) for the planar version of this problem. Equation (A2) of their appendix allows us to calculate the trajectory of a mass shell from the time it is hit by the shock until the final state of free expansion. Given this solution, their equation (A1) gives the history of the shell's density, and hence, for adiabatic flow, its sound speed $c_s(t)$. The integral of $c_s(t)dt$ gives the distance that a sound wave will travel along this mass shell during the entire period of postshock acceleration; we find $\int_{t_0(x)}^{\infty} c_s(t)dt = 1.17x$ and $2.00x$ for $n = 3$ and $n = 1.5$, respectively, where $t_0(x)$ is the time at which the shock was at the shell's initial depth x .

This indicates that the flow will remain planar as long as variations in the position and strength of the shock front occur on length scales large compared to the current depth, so that significantly different patches of the surface are out of acoustic contact. This becomes even more true if the shock is relativistic, for then the lateral region of influence is reduced in extent by a factor of about Γ_s by time dilation (e.g., Shapiro 1979). Likewise, the onset of spherical expansion causes $c_s(t)$ to drop faster than the planar solution would predict, further restricting the lateral acoustic range. In each direction this flatness criterion must be satisfied at some point as the shock approaches the stellar surface; after that, the motion is essentially planar. In reality, there are likely to be variations in the effective value of the spherical expansion factor f_{sph} , if lateral expansion sets in on the correlation scale of the flow rather than on the radial scale length R ; this would have the effect of changing the appropriate value of $x^{1/3}$. However, equation (21) shows that this variation can be ignored within the accuracy of our theory.

Secondly, what is the angular distribution of ejecta from an aspherical explosion? Sufficiently close to the outside of the star that the above criterion is satisfied, each region of the surface evolves independently of other regions separated by more than a few times the initial depth. Only one parameter controls the evolution of each region: the initial shock velocity.

Suppose that a numerical simulation has pro-

duced a shock whose intensity is p' (according to equation [15]) below a region with $d\tilde{m}_{\text{ex}}(> p')/dA$. Equation (39) can be applied to this patch of the surface, provided we replace the spherical variables $\tilde{E}_k(> \Gamma_f\beta_f)$ and $\tilde{m}_{\text{ex}}(r_{p'})$ with their differentials:

$$\frac{d\tilde{E}_k(> \Gamma_f\beta_f)}{dA} \simeq p'^{5.35\gamma_p} F(\Gamma_f\beta_f) \frac{d\tilde{m}_{\text{ex}}(> p')}{dA}; \quad (54)$$

this emission is in the normal direction. Note that here, as in (39), p' is a reference value of p and is not related to $\Gamma_f\beta_f$ by equation (22). To gain insight into the implications of equation (54) for a given explosion, we make recourse to the so-called *sector approximation*. Here, non-radial motions are ignored and each angular sector is assumed to expand as if it were part of a spherical point explosion with the local distributions of mass ($dM_{\text{ej}}/d\Omega$) and energy ($dE_{\text{in}}/d\Omega$). Equation (54), which can be re-expressed in terms of $d\Omega$ instead of dA , then states that the energy per unit solid angle above some velocity scales as $(dE_{\text{in}}/d\Omega)^{2.67\gamma_p} (dM_{\text{ej}}/d\Omega)^{1-2.67\gamma_p}$. In the simplest case, the energy and mass are those in a sector of a spherical explosion; in this case, the energy per unit area (or per unit solid angle) above some reference velocity is unchanged. In the opposite case in which all the energy is confined within some small opening angle Ω_0 , the ejecta energy above some reference velocity is increased by a factor $(4\pi/\Omega_0)^{2.67\gamma_p}$. This result gives a qualitative indication that aspherical explosions may appear far more intense (for the fortunate viewer) than spherical ones. Moreover, this effect is enhanced in an aspherical explosion in which the energy injection is concentrated in directions in which $dM_{\text{ej}}/d\Omega$ is lower than average.

Lastly, it should be noted that Chevalier (1990) and Luo & Chevalier (1994) have identified an instability of nonrelativistic, accelerating shock fronts, in which the amplitude of the perturbation doubles every four density scale heights; it saturates in a state where density is perturbed by a factor 2.5 and pressure by a factor 1.3, and oblique weak shocks follow the leading shock. These results were obtained for an exponential density profile. However, a shock in a power-law density stratification can be expected to behave similarly, except that the relevant perturbation wavelength (about two density scale heights) will shrink in

proportion to the distance to the surface, leaving behind a spectrum of artifacts in the postshock flow. To estimate whether the instability will saturate in a given star, note that the amplitude varies as $\rho^{-1/6.9}$ according to Luo & Chevalier (1994), and therefore as $\beta_s^{0.78}$. Because the shock's velocity is typically $\beta_s \sim \tilde{E}_{\text{in}}^{1/2}$ when it begins to accelerate (Matzner & McKee 1999), the density perturbation will be enhanced by a factor $\sim \tilde{E}_{\text{in}}^{-0.39}$ before the shock becomes relativistic (i.e., before $p = 1$). For the model of SN 1998bw described below, for which $\tilde{E}_{\text{in}} \simeq 0.003$, this corresponds to an amplification of one order of magnitude.

2.6. Small Ejected Masses and the Role of Gravity

Thus far, we have considered only explosions caused by the collapse of a stellar core to a much denser state; this has allowed us to neglect the binding energy of the ejected envelope, and to use equations (e.g., eq. [15]) that assume a strong point explosion. In this section we address the opposite limit: mass ejection by a shock whose total energy is small compared to the binding energy of the stellar envelope. This will allow us to analyze analytically the ejecta from collapsing compact objects.

In this limit, the shock is weak as it crosses most of the envelope, because the thermal energy of a hydrostatic envelope is comparable to its binding energy. Near the surface of the star, however, the temperature is proportional to the depth. A shock is strong if it is capable of ejecting material ($\beta_f c > v_{\text{esc}}$, the escape velocity), as the sound speed is $\sim x^{1/2} v_{\text{esc}}$. Weaker shocks are slower at any reference depth; but because they become comparable to v_{esc} closer to the surface, they are stronger (compared to the sound speed) at the point of ejection – so long as this occurs where $x \ll 1$. Although we cannot use equation (15) to predict the shock velocity from the parameters of the explosion, we can nevertheless apply our formulae for shock and postshock acceleration, and use v_{esc} to set the energy scale of what emerges.

We assume that the material of interest undergoes all of its acceleration in the vicinity of the stellar surface; then, the ejecta undergo a brief phase of acceleration followed by ballistic motion, in which they either escape ($\beta_f c > v_{\text{esc}}$)

or fall back. As relativistic stars are unstable, $E_{\text{grav}}(\text{env}) < M_{\text{env}} c^2$, so the explosions under consideration are necessarily nonrelativistic; likewise, any relativistic ejecta must escape, as v_{esc} can only be a fraction of c .

We take p to be given at some point where the shock has accelerated and become strong; thereafter, the shock (eq. [14]) and postshock (eqs. [17] and [20]) dynamics follow the theory we have developed. Under the assumption of ballistic motion, we may simply subtract the specific binding energy, $GM_*/(c^2 R) = v_{\text{esc}}^2/(2c)$, from the predicted values of Γ_f ; equivalently, the total kinetic energy in an external mass m_{ex} is reduced by $m_{\text{ex}} v_{\text{esc}}^2/2$. As this offset is less than the rest energy $m_{\text{ex}} c^2$, it clearly has no effect on ejecta with $\Gamma_f \gg 1$. However, by introducing a cutoff velocity (the escape velocity v_{esc}), it allows us to find the total kinetic energy for all the ejecta that escape. Setting $m_{\text{ex}} = M_{\text{ej}}$ and $\beta_f c = v_{\text{esc}}$ in equation (33) and subtracting $v_{\text{esc}}^2 M_{\text{ej}}/2$ from the result, we find

$$E_k \simeq \frac{3n}{5n+8} \frac{GM_*}{R_*} M_{\text{ej}}. \quad (55)$$

Insofar as Newtonian gravity remains valid, this expression is accurate to within 3% even for neutron stars.

How is the net kinetic energy in equation (55) distributed in velocity? For this, let us identify a shock intensity p_{esc} that gives $\beta_f c = v_{\text{esc}}$ via equations (14), (17), (20), and (21). If we set $p' = p_{\text{esc}}$ in equation (39), then $\tilde{m}_{\text{ex}}(> p_{\text{esc}}) = 1$, as p_{esc} determines M_{ej} ; thus,

$$E_k(> \Gamma_f \beta_f) \simeq p_{\text{esc}}^{5.35\gamma_p} F(\Gamma_f \beta_f) M_{\text{ej}} c^2, \quad (56)$$

which is valid so long as the binding energy may be neglected, i.e., $\Gamma_f \beta_f \gg v_{\text{esc}}/c$.

For a nonrelativistic escape velocity, $v_{\text{esc}} = C_{\text{nr}} f_{\text{sph}} p_{\text{esc}}$. In equation (56), when $\beta_f \ll 1$, the kinetic energy above some $\Gamma_f \beta_f$ is independent of C_{nr} and f_{sph} , as their influences on $p_{\text{esc}}^{5.35\gamma_p}$ and $F(\Gamma_f \beta_f)$ cancel. This is to be expected, as v_{esc} sets the velocity scale and $M_{\text{ej}} v_{\text{esc}}^2$ sets the energy scale (eq. [55]), and shock acceleration introduces no scales on its own, so $E_k/(M_{\text{ej}} v_{\text{esc}}^2)$ should be a pure function of $\beta_f c/v_{\text{esc}}$. These arguments no longer hold for relativistic ejecta, because the ratio v_{esc}/c becomes important, and indeed, equation (56) depends explicitly on C_{nr} and f_{sph} when

$\Gamma_f \beta_f \gtrsim 1$. With $C_{\text{nr}} = 2.03$ and $f_{\text{sph}} \simeq 0.85$, (56) becomes

$$\begin{aligned}
E_k(> \Gamma_f \beta_f) &\simeq 10^{43.53-9.72/n} \left(\frac{0.85}{f_{\text{sph}}}\right)^{5.35\gamma_p} \\
&\times \left(\frac{M_\star}{1.4 M_\odot} \frac{6000 \text{ km}}{R}\right)^{2.67\gamma_p} \\
&\times \left(\frac{M_{\text{ej}}}{0.1 M_\odot}\right) F(\Gamma_f \beta_f) \text{ erg} \quad (57a) \\
&\simeq 10^{50.96-2.29/n} \left(\frac{0.85}{f_{\text{sph}}}\right)^{5.35\gamma_p} \\
&\times \left(\frac{M_\star}{1.4 M_\odot} \frac{10 \text{ km}}{R}\right)^{2.67\gamma_p} \\
&\times \left(\frac{M_{\text{ej}}}{0.1 M_\odot}\right) F(\Gamma_f \beta_f) \text{ erg.} \quad (57b)
\end{aligned}$$

White dwarfs are sufficiently nonrelativistic that equation (57a) is a good estimate for the energetics of their ejecta. For neutron stars, the escape velocity is high enough that equation (57b) overestimates the kinetic energy of their ejecta by 15 – 30%. But, the $\sim 15\%$ uncertainty in f_{sph} causes an additional uncertainty in $E_k(> \Gamma_f \beta_f)$ of about a factor of two, for the relativistic ejecta alone.

2.6.1. Characteristic Velocities of Explosions

Equation (55) implies that, when ejecta are flung ballistically from the surface of an object and v_{esc} determines any fall-back, their mean velocity closely resembles v_{esc} , and hence $E_k \sim M_{\text{ej}} v_{\text{esc}}^2/2$. Alternatively, if E_{in} is known to exceed $M_{\text{ej}} v_{\text{esc}}^2/2$, for instance if E_{in} exceeds the binding energy of the entire stellar envelope, then it is not consistent to assume that only a small outer portion will be ejected.

In general, the explosion energy is determined at the base of the ejecta, from which it is transferred to the rest in a blast wave. Typically, the velocity scale at the base of the ejecta is the escape velocity of the forming remnant, or the infall velocity of material accreting onto it, as is clearly true for an accretion shock that ejects material by accelerating outward. Burrows (1987) and Woosley & Baron (1992) identify a neutrino-driven wind, with a velocity $\sim 0.35c$ (close to the escape velocity from a newborn neutron star), as an important possible component of core-collapse supernovae and of accretion-induced collapse in white

dwarfs; this would set an upper limit for the characteristic velocity at the base of the ejecta. In a thermonuclear explosion, the energy per nucleon prescribes a (nonrelativistic) characteristic velocity. If the remnant is a black hole, the characteristic velocity may resemble that of the last stable orbit (mildly relativistic). However, the existence of relativistic radio jets and pulsar winds indicates that magnetically-dominated outflows violate this estimate (and are typically asymmetrical). But, the postshock pressure of a blast wave driven by such a wind cannot exceed the wind’s ram pressure; this gives a lower characteristic velocity than that of the wind itself.

One implication of this inner velocity scale is that equation (14) becomes invalid near the base of the ejecta, where it predicts higher velocities because it assumes a point explosion. Another implication is that the average ejecta velocity defined by $\bar{\Gamma} = 1 + \bar{E}_{\text{in}}$ cannot exceed this characteristic inner velocity. However, the mean ejecta velocity may be much lower, because of neutrino losses, photodissociation, and work done against gravity, or simply because a relatively massive envelope is swept up.

3. Astrophysical Applications

We now consider four astrophysical examples where relativistic ejecta may result from shock and postshock acceleration caused by a violent explosion in a centrally concentrated density distribution. We use numerical simulations in tandem with our analytic approximations developed in §2. First we present a detailed model of an energetic carbon-oxygen core-collapse supernova, designed to model SN 1998bw, which has been associated with GRB 980425 (Galama et al. 1998). The progenitor density distribution is based on a model kindly provided by Stan Woosley. Next we make a simple estimate of the ejecta properties of much more extreme “hypernova” explosions in such a progenitor, and explore their ability to account for cosmological GRBs. Finally we present models of the expulsion of the outer layers of white dwarfs (WDs) and neutron stars (NSs), that undergo a hypothesized core collapse to a more compact state. The WD progenitor was generously supplied by Lee Lindblom. The density distributions of all these models are shown in Figure 7.

TABLE 1
PARAMETERS OF DENSITY MODELS

Model	\tilde{E}_{in}	A	n	f_ρ
$\rho = \rho_h x^3$	≤ 0.03	0.68	3	0.63
$\rho = \rho_h x^3$	0.1	0.72 [†]	3	0.63
$\rho = \rho_h x^3$	0.3	0.74 [†]	3	0.63
98bw ($\tilde{m}_{\text{ex}} \gtrsim 2 \times 10^{-5}$)	0.003	0.736	9	1.4
98bw ($\tilde{m}_{\text{ex}} \lesssim 2 \times 10^{-5}$)	0.003	0.736	4	0.3
WD	0.01-0.1	0.705	1.9	0.3
NS ($\tilde{m}_{\text{ex}} \gtrsim 10^{-4}$)	0.01-0.1	0.68	1.9	0.8
NS ($\tilde{m}_{\text{ex}} \lesssim 10^{-4}$)	0.01-0.1	0.68	4	0.9

[†]These values, determined by numerical simulation, are $\sim 5 - 10\%$ higher than predicted by eqs. (4), (5) and (6).

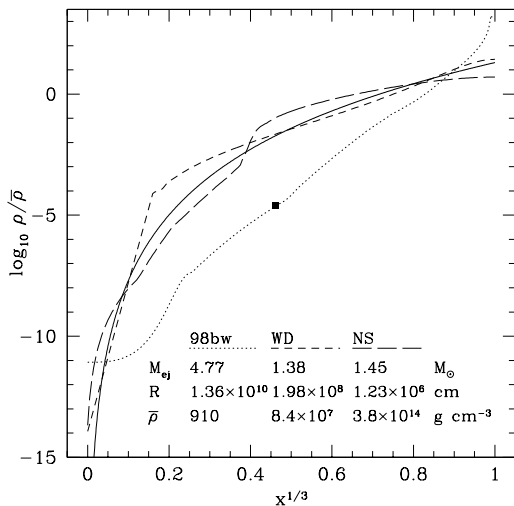


Fig. 7.— Comparison of initial density distributions of our models of SN 1998bw (*dotted*), white dwarfs (WD, *dashed*), and neutron stars (NS, *long-dashed*). The *solid* line is the idealized $\rho = \rho_h x^3$ distribution from §2. The *square* marks the location of the outer most zone considered by Woosley et al. (1999). Beyond this we extrapolate with polytropic models out to the circumstellar wind. A remnant mass of $1.78M_\odot$ has been removed from the center of this distribution, leaving $4.77 M_\odot$.

3.1. SN 1998bw and GRB 980425

SN 1998bw was a very unusual supernova. Occurring in the nearby spiral galaxy ESO 184-G82 at $z = 0.0085$, equivalent to 38 Mpc for $H_0 = 65 \text{ km s}^{-1} \text{ Mpc}^{-1}$ (Tinney et al. 1998), it is one of the most luminous and earliest peaking Type Ib/c radio supernovae ever observed (Li & Chevalier 1999; Weiler et al. 2000): its maximum radio luminosity was $\sim 4 \times 10^{38} \text{ ergs s}^{-1}$, occurring 12 ± 2 days after core-collapse (Kulkarni et al. 1998). Various authors have derived differing shock expansion velocities from synchrotron models of this emission, finding $\beta_s \sim 0.3 - 0.8$ about 12 days after the start of the supernova (Kulkarni et al. 1998; Waxman & Loeb 1999; Li & Chevalier 1999). The more relativistic the expansion, the greater the chance that γ -rays could have been produced immediately after the star exploded. We shall consider these models further in §3.1.3, where we compare them to our predictions from the distribution of high-velocity ejecta.

Because of the lack of H and He I features in its optical spectrum, SN 1998bw has been classified as a peculiar Type Ic event (Patat & Piemonte 1998). The optical spectra also reveal very broad emission line blends of Fe II, Si II, O I, and Ca II, implying very high expansion velocities $\sim 0.2c$ about a week after the explosion. The peak optical luminosity ($\sim 1 \times 10^{43} \text{ ergs s}^{-1}$) is about ten times brighter

than typical SNe Ib/Ic. Modeling SN 1998bw’s spectra and light curve under the assumption of a spherically symmetric explosion of a C+O star, with $M_{\text{ej}} \sim (5 - 10) M_{\odot}$, requires large synthesized Ni masses ($\gtrsim 0.5 M_{\odot}$) and explosion kinetic energies ($\sim (2 - 5) \times 10^{52}$ ergs) (Iwamoto et al. 1998; Woosley et al. 1999; Sollerman et al. 2000; Nakamura et al. 2000), again about an order of magnitude greater than from typical supernovae. However, Höflich et al. (1999) have presented asymmetric explosion models that require smaller energies.

GRB 980425 also has some unusual properties distinguishing it from other bursts. Observed by the BATSE detector on the *Compton Gamma Ray Observatory* (Bloom et al. 1998a) and the *Beppo-SAX* satellite (Soffitta et al. 1998), no emission was seen above 300 keV, making this an example of the “no high energy” bursts that compose $\sim 25\%$ of the BATSE sample. The burst profile was smooth and single peaked, showing little internal variability. At most, only seven other bursts (0.5% of the total GRB population) display such profiles (Norris, Bonnell, & Watanabe 1999). The burst duration, t_b , was about 35 s, with the count rate of photons above 40 keV peaking four or five seconds before the count rate of photons below 26 keV (Pian et al. 2000). Pian et al. also report that the supernova is coincident with an X-ray source that fades by a factor of two over the first six months.

However, the most intriguing aspect of the unusual events SN 1998bw and GRB 980425 is their spatial and temporal association (Galama et al. 1998), occurring with $\lesssim 10^{-4}$ chance probability according to *a posteriori* statistics. Their peculiarities only serve to strengthen the suspicion that they are related. Given association, the γ -ray energy of the burst was $E_{\gamma} = (8.1 \pm 1.0) \times 10^{47}$ ergs, equivalent to $\sim 10^{27} \text{ g } c^2$. Such a weak burst, thousands to millions of times fainter than the inferred isotropic energies of cosmological bursts, implies a separate GRB population. Corroborating this suspicion, Norris, Marani, & Bonnell (2000) have shown that there is a power law anticorrelation between intrinsic luminosity and hard-to-soft time lags among six other bursts with known redshifts, but that GRB 980425, if associated with SN 1998bw, is several hundred times weaker than this law would predict. Moreover, Hogg & Fruchter (1999) have shown that if the

rate at which GRBs occur within a galaxy is proportional to its luminosity, then the odds of detecting a burst at redshift $z = 0.0085$ in the current sample of GRBs with known redshifts are less than one in 10^4 . Non-Euclidean number count statistics limit the fraction of observed bursts resulting from this mechanism to $\lesssim 10\%$ (Bloom et al. 1998a).

3.1.1. Relativistic Ejecta from SN 1998bw

We wish to examine in detail the question of whether the relativistic ejecta from SN 1998bw were plausibly sufficient to power GRB 980425. Previous estimates of the mass and energy associated with relativistic supernova ejecta have extrapolated nonrelativistic results to the relativistic regime; in this manner, Matzner & McKee (1999) predicted sufficient energy in relativistic motion to account for the gamma-ray burst. Woosley et al. (1999) simulated shock break-out from a variety of progenitor models for SN 1998bw with ejected masses in the range $5 - 12 M_{\odot}$ and explosion energies $(4 - 28) \times 10^{51}$ ergs. Our investigation of SN 1998bw will be restricted to Woosley et al.’s model CO6, which Stan Woosley has kindly provided us. This is the bare carbon-oxygen core ($\sim 6.6 M_{\odot}$) of a star that was initially more massive ($\sim 25 M_{\odot}$); its pre-explosion luminosity is $6.6 \times 10^{38} \text{ ergs s}^{-1}$. The supernova forms a neutron star of $1.78 M_{\odot}$ and ejects $4.77 M_{\odot}$ with 28×10^{51} ergs (Table 2). It is the most energetic explosion in the most compact, lowest mass progenitor considered by Woosley et al. (1999). Among their models for the supernova’s explosion, they find it gives the best fit to the observed bolometric and spectroscopic light curves; however, significant discrepancies, such as the fast observed rise in its luminosity, remain.⁵

Woosley et al. (1999) used a nonrelativistic code with logarithmically smooth zoning down to $10^{-6} M_{\odot}$. Estimating the energetics of the radiation flash associated with shock break-out, they concluded it was far too weak (10^{42-46} erg) to power the GRB. Woosley et al. (1999) also estimated the amount of relativistic mass ejection, by extrapolating their simulation to small masses with the shock acceleration formula of Gnatyk

⁵Iwamoto et al. (1998) favor a more massive ($M_{\text{ej}} \sim 10 M_{\odot}$) progenitor, with a correspondingly more energetic (up to $\sim 5 \times 10^{52}$ ergs) explosion, giving similar values for \dot{E}_{in} .

TABLE 2
SN 1998BW MODEL PARAMETERS

M_*	$6.55 M_\odot$
M_{rem}	$1.78 M_\odot$
M_{ej}	$4.77 M_\odot$
E_{in}	2.8×10^{52} ergs
R	1.40×10^{10} cm

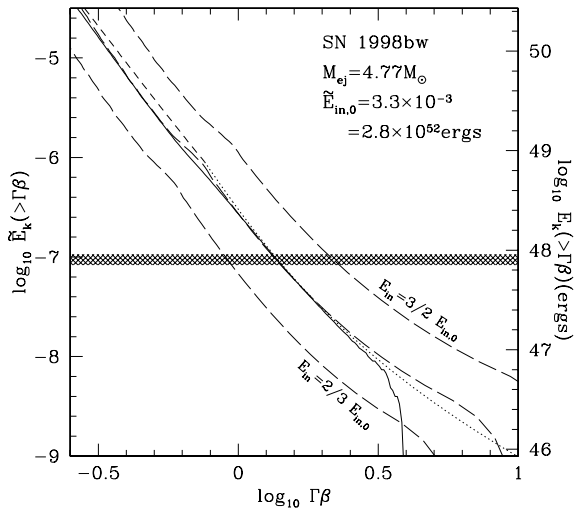


Fig. 8.— Cumulative kinetic energy distribution of ejecta for SN 1998bw from simulation (*solid* line) and theory: the central *long dashed* line is numerical integration of equation (29) over the progenitor density distribution, with Γ_f predicted from equations (15), (14), (17) and (21); the upper and lower *long dashed* lines show the effect of increasing and decreasing the initial energy by a factor of 1.5, for this method; predictions from equation (37) are shown by the *dotted* ($n = 4$, $f_\rho = 0.3$, fit to outer ejecta) and *dashed* ($n = 9$, $f_\rho = 1.4$, fit to inner ejecta) lines. The *hatched* area shows the uncertainties in the observed γ -ray energy of GRB 980425.

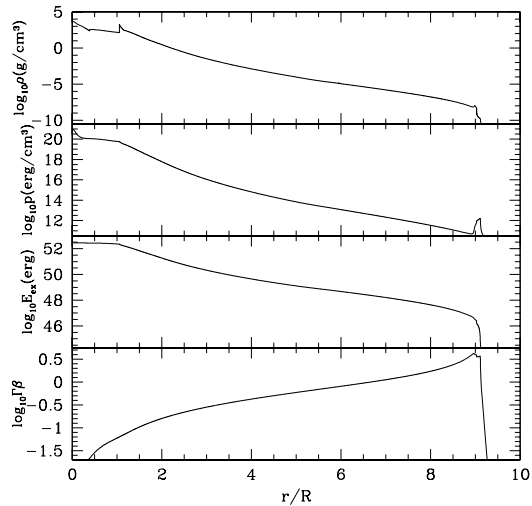


Fig. 9.— Density, pressure, energy (E_{ex}), and specific momentum ($\Gamma\beta$) of the ejecta from simulated supernova explosion CO6, after expansion to $9 R$ into a wind whose mass loss rate is $\dot{M}_w = 10^{-5} M_\odot \text{ yr}^{-1}$. E_{ex} is the kinetic + thermal energy external to a particular location. The reverse shock due to the circumstellar interaction is visible in the distributions of density, pressure and velocity.

(1985), given here as equation (8). On this basis, they estimated $10^{44} - 10^{45}$ ergs in kinetic energy of material with $\Gamma > 3$ and $10^{41} - 10^{42}$ ergs for $\Gamma > 10$. However, as trans-relativistic postshock acceleration (§2.2) was not included, and as we have improved upon Gnatyk’s formula in §2, we wish to re-examine the topic of relativistic ejection from model CO6.

There are four methods we may employ to execute this investigation. First, knowing the mass, radius, luminosity and composition of the progenitor, we may use the analytical predictions of §2.4 to give $E_k(\Gamma_f \beta_f > 1)$. For this progenitor, bound-free absorption dominates in an outer mass M_{rel} . Equation (49), which neglects radiation pressure, predicts $M_{\text{rel}} \simeq 0.99 \times 10^{27}$ g with kinetic energy $E_k(> 1) \simeq 8.0 \times 10^{47}$ erg. In fact as the luminosity of CO6 is about a quarter of the (electron-scattering) Eddington limit, radiation pressure is not negligible, $n > 3.25$ and the above estimates are lower limits.

Second, if the outer density distribution of the progenitor were well fit by a power-law density ramp (eq. [23]), then with the fiducial explosion parameters of Table 2, we could evaluate M_{rel} and $E_k(> 1)$ directly from equations (43) and (42). However, for model CO6 no single pair of values for n and f_ρ accurately describe the whole of the outer region. In particular the structure changes around $m_{\text{ex}} \sim 1 \times 10^{-4} M_\odot$. The layers just interior to this point are well described by $n \simeq 9$ and $f_\rho \simeq 1.4$, while exterior we find $n \simeq 4$ and $f_\rho \simeq 0.3$. To obtain the energy distribution as a function of velocity, $E_k(> \Gamma\beta)$, we employ equation (37) with $A = 0.736$, motivated by equations (4) and (5), and the interior power-law fit ($n = 9, f_\rho = 1.4$). Internal variations in the density structure effect the accuracy of this normalization of E_k . Beyond the location where the structure changes to the $n = 4$ case we extrapolate using equation (40). This “broken power-law” estimate is shown by the *dashed* and *dotted* lines in Figure 8. By this method we find $E_k(> 1) \simeq 2.5 \times 10^{48}$ erg and, from equation (43), $M_{\text{rel}} \simeq 3.0 \times 10^{27}$ g.

A third, more accurate, method is possible: since we have the full density distribution of the progenitor model, we may directly apply equations (14), (17), and (21) to obtain the distribution of ejecta at all velocities sufficiently fast for these equations to hold. This technique accounts for in-

terior density variations, which affect the nonrelativistic shock propagation and thus the normalization of the broken power-law estimate, which is based solely on the structure of the outer layers. Applying this more detailed approach is complicated by the fact that the outermost zone of model CO6 is about 2×10^{27} g in mass; this is the same order of magnitude as the estimates of M_{rel} identified above. For accurate estimates, it is clearly necessary to continue the sub-surface density distribution to much lower values. We therefore extrapolate model CO6 using a power-law atmosphere with $n = 4$, matched to the outer edge of the original model. After this extrapolation, the smallest zone of the stellar model has a mass of $10^{-9} M_\odot$, several thousand times smaller than M_{rel} ; yet, this zone is still optically thick to the high energy photons that drive the outward shock (a necessity for it to participate in shock acceleration; Matzner & McKee 1999). We find that our results for the mildly relativistic ejecta are not very sensitive to our choice of n , nor to the exact value of the minimum zone mass. Applying equations (14), (17), and (21) to the augmented progenitor model, we find $M_{\text{rel}} = 3.9 \times 10^{27}$ g and $E_k(> 1) = 2.1 \times 10^{48}$ erg. These values are within $\pm 30\%$ of those obtained above by power-law fits. The full energy distribution is shown by the central *long dashed* line in Figure 8. The upper and lower *long dashed* lines show the cases of $E_{\text{in}} = 4.2 \times 10^{52}$ and 1.9×10^{52} ergs, i.e. increasing and decreasing the fiducial explosion energy by a factor of 1.5.

The final and most authoritative method to determine M_{rel} and $E_k(> 1)$ is by direct numerical simulation. Following Woosley et al. (1999), we simulate the explosion of CO6 by subtracting a remnant mass of $1.78 M_\odot$ from the center and depositing $E_{\text{in}} = 2.8 \times 10^{52}$ ergs in several pressurized, stationary zones; ignoring the effects of gravity, we follow the subsequent behavior until the final state of free expansion (for the relativistic ejecta, $r > 9R$ suffices). We embed the progenitor in an optically thick stellar wind described by the models of Springmann (1994) (see also Heger & Langer 1996), considering mass loss rates of 10^{-6} , 10^{-5} and $10^{-4} M_\odot \text{ yr}^{-1}$. The wind velocities are relatively low near the boundary of the star, increasing smoothly to achieve 90% of the terminal velocity, v_w , within $10 - 25 R$. Heger

& Langer (1996) set v_w equal to the escape velocity from the stellar surface, which gives a velocity of $3.6 \times 10^8 \text{ cm s}^{-1}$ for our progenitor. We note this estimate of v_w is uncertain and observed velocities from WC stars are about a factor of two lower (Koesterke & Hamann 1995). However, we find that the detailed structure of the stellar wind is of little consequence in our simulations of the explosion. After the outermost ejecta have expanded to $9 R$ their thermal energy has dropped to only a few percent of their kinetic and postshock acceleration is essentially complete. At this point, only $\sim 10^{-8} M_\odot$ has been affected by the reverse shock caused by its interaction with the wind (see Figure 9). This justifies the approximation employed by Matzner & McKee (1999), and also in §2 above, that the production of high-velocity ejecta is unaffected by the existence of circumstellar material. We shall argue in §§3.1.2 and 3.1.3 that GRB 980425 and the radio emission from SN 1998bw were due to the circumstellar interaction; however, this occurs at much larger radii, where the wind has reached its terminal velocity.

Our numerical simulation places 2.3×10^{48} ergs in 4.1×10^{27} g with $\Gamma_f \beta_f > 1$, in excellent agreement with the values predicted by our shock and postshock theory (i.e., the third method listed above). The energy distribution of the simulation is shown in Figure 8 by the *solid* line. We conclude that our equations describing the shock speed and the postshock acceleration of trans-relativistic ejecta do an excellent job of predicting its energy distribution with velocity – except, of course, for material that has been swept into the reverse shock ($\log_{10}(\Gamma_f \beta_f) > 0.6$). The upper and lower limits for the observed γ -ray energy of GRB 980425, assuming it was associated with SN 1998bw, are shown by the *hatched* area in Figure 8. For our fiducial model, we predict ejecta traveling faster than $\Gamma\beta \gtrsim 1.35$, corresponding to a velocity $\beta \gtrsim 0.8$, have $E_k = E_\gamma$. Note that an explosion with twice our fiducial energy in a $10 M_\odot$ progenitor, as considered by Iwamoto et al. (1998), has the same value of \dot{E}_{in} , but results in $E_k(> \Gamma\beta)$ twice as large at any given velocity, assuming the same density structure.

Compared to Woosley et al. (1999), we find two to three orders of magnitude more energy in ejecta traveling at mildly relativistic ($\Gamma_f \sim 3$) velocities. This is principally because of our inclusion

of trans-relativistic postshock acceleration, which boosts the final $\Gamma\beta$ of the ejecta by a factor of $\sim [2 + (\Gamma_s \beta_s)^{\sqrt{3}}]$. The steeply declining density gradient of the progenitor, with $n = 4$, results in $E_k(> \Gamma_f \beta_f) \propto (\Gamma_f \beta_f)^{-4.6}$ (eq. 35) in the nonrelativistic limit – a very rapid falloff with velocity. Increasing the final velocities of *all* the outer ejecta by even a modest factor significantly increases the kinetic energy above a *particular* $\Gamma_f \beta_f$. While we find enough energy in mildly relativistic ejecta to account for the energetics of GRB 980425, the ultrarelativistic ejecta are too puny to be of consequence. We now examine if a mildly relativistic explosion can explain the observed gamma-ray burst and radio supernova.

3.1.2. Early Evolution - Gamma-Ray Burst

We assume γ -rays are produced with efficiency ϵ_γ as the kinetic energy from relativistic ejecta is released on collision with an effectively stationary circumstellar wind. For a mass m_{ex} of ejecta traveling at a (mass-weighted) mean Lorentz factor $\bar{\Gamma} \equiv 1 + E_k(m_{\text{ex}})/(m_{\text{ex}}c^2)$, about half of the initial kinetic energy $E_k(m_{\text{ex}})$ will be liberated after a mass $\sim m_{\text{ex}}/\bar{\Gamma}$ of circumstellar matter has been swept up (e.g., Piran 1999). This estimate is based on energy and momentum conservation in the wind frame, assuming adiabatic interaction. Accounting for energy radiated away, leads to less wind material being required. For a wind of constant velocity v_w and mass loss rate \dot{M}_w , the mass contained in a sphere of radius $r \gg R$ around the star is $M_w = \dot{M}_w r / v_w$. Therefore, to liberate an amount of kinetic energy E_γ requires an interaction with the wind material out to the radius

$$r(E_\gamma) \simeq \frac{E_\gamma v_w}{\epsilon_\gamma \bar{\Gamma} (\bar{\Gamma} - 1) \dot{M}_w c^2}, \quad (58)$$

where ϵ_γ cannot be much greater than a half.

Let us suppose that the shocked shell driven outward by the ejecta mass m_{ex} travels with mean Lorentz factor Γ_{shell} ; this is also the Lorentz factor of the shock that entrains the wind, if it is fully radiative. Ignoring the fact that this shell decelerates, the time for it to reach radius r is $t' \simeq r/(\beta_{\text{shell}}c)$ in the wind's frame. However, the observed time of the burst, t'_{obs} ⁶, is shorter by a

⁶ $t'_{\text{obs}} = t_{\text{obs}}/(1+z)$, where t_{obs} is the actual observed time at Earth and z is the redshift of the burst.

factor $1 - \beta_{\text{shell}}$ (still ignoring deceleration), so that

$$r(t'_{\text{obs}}) \simeq \frac{ct'_{\text{obs}}}{\beta_{\text{shell}}^{-1} - 1} \simeq 2\Gamma_{\text{shell}}^2 ct'_{\text{obs}}. \quad (59)$$

Here, the approximation $\beta_{\text{shell}}^{-1} - 1 \simeq 1/(2\Gamma_{\text{shell}}^2)$ overestimates $r(t'_{\text{obs}})$ for trans-relativistic motions (for instance, by 37% when $\Gamma_{\text{shell}} = 1.7$), but this should roughly compensate for our neglect of the shell's deceleration, which causes us to underestimate $r(t'_{\text{obs}})$.

What is the relationship between the Lorentz factor of the shell ($\Gamma_{\text{shell}}(r)$), the mean Lorentz factor of the ejecta that has struck the shell ($\bar{\Gamma}(r)$), and the Lorentz factor of ejecta currently striking the shell ($\Gamma_f(r)$, say)? We must have $\bar{\Gamma}(r) > \Gamma_f(r)$ because slower ejecta collide with the shell at later times. In fact, $\Gamma_f(\bar{\Gamma}) = \Gamma_f(E_k)$ is given by the ejecta's energy distribution, e.g., by equation (37); for instance, we find that to have $\bar{\Gamma} = 2$ requires $\Gamma_f \simeq 1.7$, for a variety of values of n . Also, $\Gamma_{\text{shell}} < \Gamma_f$, because the ejecta must be able to catch up with the shell. However, we expect that the latter quantities differ by a relatively small amount.

The total isotropic energy of GRB 980425 in photons above 24 keV, assuming association with SN 1998bw, is $E_\gamma = (8.1 \pm 1.0) \times 10^{47}$ ergs; its observed duration is $t_{\text{obs}} \sim 35$ s and this is approximately equal to t'_{obs} , because the redshift is negligible. Requiring that $r(t'_{\text{obs}}) = r(E_\gamma)$ in equations (58) and (59) gives the following estimate of the wind's mass loss rate:

$$\frac{\dot{M}_{-4}}{v_{w,8}} \sim \frac{3}{(\bar{\Gamma} - 1)(\bar{\Gamma}/2)(\Gamma_{\text{shell}}/1.7)^2} \times \left(\frac{\epsilon_\gamma}{0.5}\right)^{-1} \left(\frac{E_\gamma}{10^{48} \text{ erg}}\right) \left(\frac{t'_{\text{obs}}}{35 \text{ s}}\right)^{-1}, \quad (60)$$

where $\dot{M}_{-4} = \dot{M}_w/10^{-4} M_\odot \text{ yr}^{-1}$ and $v_{w,8} = v_w/10^8 \text{ cm s}^{-1}$.

In our fiducial model for SN 1998bw, we find ejecta with $\bar{\Gamma} \simeq 2$ and $\Gamma_f \simeq 1.7$ carry an energy equal to E_γ . Ejecta with $\bar{\Gamma} \simeq 1.6$ and $\Gamma_f \simeq 1.4$ contain a few $\times 10^{48}$ ergs. If we take $\Gamma_{\text{shell}} \sim \Gamma_f$ and $v_w \sim 10^8 \text{ cm s}^{-1}$, equation (60) indicates that pre-supernova mass loss rates of order a few $\times 10^{-4} M_\odot \text{ yr}^{-1}$ are required to explain the observed 35 s duration of GRB 980425. Note that the radius of the circumstellar interaction is about 400 R , far outside the region in which the wind undergoes its acceleration (Springmann 1994).

Wolf-Rayet stars have mass loss rates typically in the range $10^{-6} - 10^{-4} M_\odot \text{ yr}^{-1}$ (Hamann, Koesterke, & Wessolowski 1995). However, it is interesting that those in the carbon-rich (WC) subclass are at the high end of this range. Koesterke & Hamann (1995) present observations of 25 WC stars, with a mean mass loss rate of $\sim 6 \times 10^{-5} M_\odot \text{ yr}^{-1}$ and about one order of magnitude dispersion. To produce GRB 980425 from the mildly relativistic ejecta emerging from SN 1998bw, we conclude that the circumstellar medium be dense but within the range observed around Wolf-Rayet stars.

While a dense circumstellar environment is necessary to liberate the relativistic kinetic energy of the ejecta, it should be checked that the γ -rays thus produced can escape this region to be observed at Earth. For this we calculate the photospheric radius, R_p , outside of which the γ -ray optical depth is $\tau = 2/3$:

$$\tau = \frac{2}{3} = f_{\text{kn}} \kappa_{\text{es}} \int_{R_p}^{\infty} \rho_w dr = \frac{\dot{M}_w f_{\text{kn}} \kappa_{\text{es}}}{4\pi v_w R_p}. \quad (61)$$

Here, $\kappa_{\text{es}} = 0.40/\mu_e \text{ cm}^2 \text{ g}^{-1}$, where $\mu_e = 2/(1 + X_H) \simeq 2$ is the mean molecular weight per electron, and f_{kn} is the relativistic (Klein-Nishina) correction to the Thompson cross section; $f_{\text{kn}} = 0.53, 0.74, 0.84$ for γ -rays of energy 300, 100, 50 keV. Thus, we have

$$R_p = 1.5 \times 10^{12} f_{\text{kn}} \frac{\dot{M}_{-4}}{v_{w,8}} \text{ cm}, \quad (62)$$

Although this photospheric radius ($\sim 100R$) is much bigger than the star, it is not larger than the interaction radius $r(E_\gamma) = r(t'_{\text{obs}}) \sim 400R$ identified above, implying that the GRB will indeed be visible. Additionally, equation (62) predicts smaller photospheric radii and earlier emergence for higher energy photons because of the energy dependence of the Klein-Nishina opacity. For typical conditions inside R_p these higher energy photons are expected to be present (Weaver 1976), and indeed the observed lightcurves of GRB 980425 peak a few seconds earlier for higher (> 40 keV) energies than for lower (< 26 keV) energies (Pian et al. 2000).

As the emphasis of this paper is on the energetics of relativistic mass ejection, we shall not attempt to calculate in any detail the spectrum

of the observed outburst; however, note that the typical energies of these photons will depend on the mechanism of their emission. Non-thermal processes include inverse Compton upscattering of lower energy photons, or synchrotron emission by electrons produced in the shock front. As the latter is the canonical mechanism for the emission from GRBs, we give a simple estimate of the typical energies of these photons. Consider a shock of Lorentz factor Γ_{sh} propagating into the wind (density $\rho_w = \dot{M}_w/(4\pi r^2 v_w)$). The postshock Lorentz factor Γ_2 is related to Γ_{sh} by equation (16). The postshock energy density (Blandford & McKee 1976), minus the rest energy of the postshock fluid, is the energy density associated with the postshock pressure:

$$e_2 - \rho_2 c^2 = (4\Gamma_2 + 3)(\Gamma_2 - 1)\rho_w c^2. \quad (63)$$

Following Piran (1999), we assume that electrons and magnetic fields account for fractions ϵ_e and ϵ_b of this amount, respectively. The typical random Lorentz factor of an electron in the postshock flow is then

$$\bar{\gamma}_e = \frac{\mu_e M_p}{M_e} \epsilon_e (\Gamma_2 - 1). \quad (64)$$

Approximating $\Gamma_{\text{shell}} \simeq \Gamma_2$, and evaluating the photon energy of synchrotron radiation by a typical electron at the radius $r(t'_{\text{obs}})$ given in equation (59), we find

$$\begin{aligned} h\nu_{\text{syn}} &\simeq 6.3\mu_e^2 \Gamma_{\text{shell}} (\Gamma_{\text{shell}} - 1)^{1/2} (4\Gamma_{\text{shell}} + 3)^{1/2} \\ &\times \epsilon_e^2 \epsilon_b^{1/2} \left(\frac{\dot{M}_{-4}}{v_{w,8}} \right)^{1/2} \left(\frac{t'_{\text{obs}}}{35 \text{ s}} \right)^{-1} \text{ keV}. \end{aligned} \quad (65)$$

With $\mu_e \simeq 2$, this gives $h\nu_{\text{syn}} \simeq (8, 14, 29, 73) \times (\epsilon_e/0.5)^2 (\epsilon_b/0.5)^{1/2} (35 \text{ s}/t'_{\text{obs}}) \dot{M}_{-4}/v_{w,8}$ keV, for $\Gamma_{\text{shell}} = (1.25, 1.5, 2, 3)$. The synchrotron model is thus roughly consistent with the photon energies observed in the burst. It suggests that the softening of these photons over time may have been caused by the shell's deceleration combined with the declining pre-shock density.

The earlier arrival of harder photons thus occurs naturally in both the optically thick regime, because R_p is a decreasing function of $h\nu$, and in the optically thin regime, because of the decline in $h\nu_{\text{syn}}$ as the shell expands.

3.1.3. Late Evolution - Radio Supernova

Radio observations of SN 1998bw have been used to infer ejecta expansion velocities, assuming the radio emission originates in a shell just behind the forward shock as it propagates into the stellar wind. Kulkarni et al. (1998) argued the lack of strong variability at low frequencies implies the shock reached a size $\gtrsim 10^{16}$ cm, set by the refractive scintillation scale of the Galactic ISM, by the time of the radio light curve peak at ~ 12 days. This implies $\bar{\beta}_s \gtrsim 0.3$ averaged over this period. Furthermore, Kulkarni et al. (1998) pointed out that two constraints, one on the brightness temperature limited by inverse Compton scattering and the other on the total energy of a synchrotron emitting source, require relativistic ($\Gamma\beta \sim 1.6 - 2$) shock expansion velocities up to 60 days after the start of the supernova explosion.

Waxman & Loeb (1999) and Li & Chevalier (1999) have presented additional models of the radio emission. Waxman & Loeb (1999) considered a mono-energetic, approximately thermal, electron energy distribution, to derive shock expansion with $\beta_s \sim 0.3$ at $t = 12$ days. They argued the radio emission does not imply the presence of a highly relativistic blast wave and that this weakens the link between SN 1998bw and GRB 980425. Their model required only a weak magnetic field, far from equipartition, and a high density ($\sim 10^4 - 10^5$) of emitting electrons. Li & Chevalier (1999) modeled a power law electron energy distribution and accounted for effects of relativistic expansion of the synchrotron source. They derived a range of values of the total energy, equipartition fractions of electrons, ϵ_e , and magnetic fields, ϵ_b , and the ambient wind density that were compatible with the radio observations. They considered a specific, arbitrary model with $\epsilon_b = 10^{-6}$ and a dense ($\dot{M}_{-4}/v_{w,8} = 0.6$) wind, which gave $\Gamma_s \beta_s \sim 0.75$ after 12 days.

How do the above velocities compare to those predicted from our model? The circumstellar interaction becomes nonrelativistic after a wind mass $\sim M_{\text{rel}}$ has been swept up; this happens at a radius $r \gtrsim 10^{14} v_{w,8}/\dot{M}_{-4}$ cm, or after about one hour has elapsed since the burst. The shock is therefore non- or mildly relativistic ($\Gamma_{\text{shell}} \simeq 1$) at the time of the radio observations. We assume the forward, radiating shock expands according to

$r_s \propto t^\eta$, so that $\beta_s c = \eta r/t$ where $0 < \eta < 1$. The ejecta colliding with the shocked shell are in free expansion ($\beta_f c = r/t$), so $\beta_s = \eta \beta_f$. The nonrelativistic ejecta are distributed as $\rho_f \propto \beta_f^{l_{\rho 2}}$, where $l_{\rho 2} \simeq -(8.3 + 5.3/n)$ (e.g., Matzner & McKee 1999). Because $l_{\rho 2} < -5$, the self-similar solution of Chevalier (1982) and Nadyozhin (1985) applies: there, the ratio of masses of shocked ejecta and ambient material is a constant. Fitting the data in Chevalier’s table, we find

$$\frac{m_{\text{ex}}}{M_w} = \frac{-l_{\rho 2}}{2.7} - 1.8, \quad (66)$$

within four percent. The expansion parameter η is determined by the requirement that the ratio m_{ex}/M_w be constant:

$$\eta = \frac{n + 1}{1.2n + 1}. \quad (67)$$

Note that the deceleration is very slow ($\eta \simeq 1$); this will be crucial to the persistence of rapid expansion into the epoch of the radio observations.

Requiring that the ambient mass within r and the ejecta mass traveling faster than $\beta_f = \beta_s/\eta$ satisfy equation (66), and using equations (3), (17), (19), and (23) to specify $M_{\text{ej}}(> \beta_f)$, we find that for our fit ($n = 4$, $f_\rho = 0.3$) to the outer envelope,

$$\beta_{\text{shell}} \simeq 0.42 \left(\frac{E_{\text{in}}}{2.8 \times 10^{52} \text{ ergs}} \right)^{0.43} \left(\frac{v_{w,8}}{M_{-4}} \right)^{0.13} \times \left(\frac{M_{\text{ej}}}{4.77 M_\odot} \right)^{-0.30} \left(\frac{t}{1 \text{ day}} \right)^{-0.13}. \quad (68)$$

After twelve days $\beta_s \simeq 0.30$; the velocity declines only slowly because the amount of ejecta mass traveling faster than a given β_f increases steeply as β_f decreases. The average velocity is faster by only 15%, due to the slowness of the deceleration, so the mean rate of expansion is $\bar{\beta}_s = 0.35$ at twelve days. This velocity satisfies the constraints from the radio scintillation measurements, and is consistent with synchrotron emission models, given their uncertainties, e.g. in the assumed electron distribution. Including relativistic effects would not much alter our result because these have two counteracting effects: on the one hand, they increase the final velocities of ejecta, thus raising the velocity relative to the above equation; but on

the other, they lead to a smaller swept-up mass being required to slow down the ejecta, thus reducing the velocity.

We conclude that an energetic spherical explosion of a few $\times 10^{52}$ ergs in a compact, relatively low mass carbon-oxygen core of a massive star is capable of producing enough relativistic ejecta to account for the energetics of GRB 980425. The results of Woosley et al. (1999) favor this type of progenitor from fits to the light curve and spectra, although the explosion energy we require is at the high end of the range they considered. The timescale of the burst requires a relatively dense stellar wind around the CO core, with implied mass loss rates $\sim \text{few} \times 10^{-4} M_\odot \text{ yr}^{-1}$. Gamma-ray photons are able to escape from this wind to be observed at Earth. Note that opacity due to photon-photon interactions (see §3.2) does not constrain the minimum Lorentz factor of the ejecta because the observed GRB spectrum is very soft. These typical wind densities also allow γ -rays of the correct energy to be produced by synchrotron emission behind the mildly relativistic forward shock. The shock velocity into this dense wind is fast enough to explain the radio properties of SN 1998bw days after the GRB. This simple spherical model is thus able to account for the observed properties of GRB 980425, if indeed it was associated with SN 1998bw.

3.2. Hypernovae and Cosmological Gamma-Ray Bursts

In §3.1 we found that GRB 980425 and the radio afterglow of SN 1998bw can plausibly be attributed to the collision of mildly relativistic ejecta with a circumstellar wind. An interaction of this type has often been considered as an important possibility for GRB afterglows (Rees & Mészáros 1998; Panaitescu, Mészáros, & Rees 1998; Sari & Mészáros 2000). External shock models have also been proposed (Mészáros & Rees 1993) for the emission from cosmological GRBs; however, these have been criticized (e.g., Sari & Piran 1997; Piran 1999) on the basis that they cannot reproduce the substructure observed in many GRBs. This constraint does not apply to GRB 980425, whose profile was smooth, nor to the few other bursts (Norris, Bonnell, & Watanabe 1999) that share this property. Could cosmological bursts with smooth γ -ray light curves be produced by

TABLE 3

CONSERVATIVE LOWER LIMITS ON Γ IN THE EXTERNAL SHOCK MODEL FOR GRBs WITH AFTERGLOWS

GRB	Redshift, z	Isotropic E_γ (10^{52} erg)	Duration (s) $t_{\text{obs}} = t'_{\text{obs}}(1+z)$	Min. $\bar{\Gamma}$ (eq. 71) [external opacity]	Min. $\bar{\Gamma}$ (eq. 69; $\alpha = 2$) [$\gamma - \gamma$ opacity]	Refs. ^a
970228	0.695	0.5	80	9	9	1, 2, 3
970508	0.835	0.8	15	17	14	3, 4
971214	3.418	30	25	36	25	5, 6
980703	0.966	10	100	14	12	7, 8
990123	1.600	300	100	28	20	9, 10
990510	1.619	30	80	20	15	3, 11
991208	0.706	13	60	17	14	12, 13
000301C	2.03	0.2	10	19	15	14, 15
000418	1.119	4.9	30	15	13	16, 17
000926	2.066	26	25	31	22	18, 19

^aTable is based on data compiled by J. Greiner and S. Hempelmann at www.aip.de/~jcjg/grbrsh.html. (1) Costa & Feroci (1997); (2) Djorgovski, Kulkarni, & Bloom (1999); (3) Harrison et al. (1999); (4) Costa et al. (1997); (5) Heise & in 't Zand (1997); (6) Mészáros (1999); (7) from <http://gamma-ray.msc.nasa.gov/batse/grb/lightcurve/>; (8) Bloom et al. (1998b); (9) Feroci et al. (1999); (10) Kulkarni et al. (1999); (11) Dadina et al. (1999); (12) Hurley & Cline (1999); (13) Djorgovski et al. (1999b); (14) Smith, Hurley, & Cline (2000); (15) Castro et al. (2000); (16) Hurley, Cline & Mazets (2000); (17) Bloom et al. (2000a); (18) Hurley et al. (2000); (19) Fynbo et al. (2000).

spherical explosions of over-energetic supernovae (“hypernovae”; Woosley 1993; Paczynski 1998), in the same manner that GRB 980425 was produced by SN 1998bw?

The cosmological GRBs with known redshifts require explosion energies of $10^{51.5-54.5}$ erg, i.e., $(0.002 - 2) \times M_\odot c^2$ to be emitted as γ -rays, under the assumption of isotropic emission. By extracting energy efficiently from the formation of a massive black hole at its center, a hypernova may be capable of such energies. (Note that the stellar-mass Galactic black holes are clustered around $7 M_\odot$; Bailyn et al. 1998). However, in a spherical explosion of the type advocated for SN 1998bw, much of the energy is locked up in ejecta moving near the mean Lorentz factor $(1 + \bar{E}_{\text{in}})$. It is well known that the time scales and energies of GRBs require significant Lorentz factors to be optically thin; this would imply an even larger energy in low-velocity ejecta, if the necessary value of Γ significantly exceeds $1 + \bar{E}_{\text{in}}$.

There are two potential sources of opacity that can shade GRB emission, and hence two constraints on the Lorentz factor. The first of these is absorption of the observed photons in pair-

producing interactions with other photons (Krolik & Pier 1991; Baring & Harding 1997); this leads to the “compactness problem” for GRBs. The cross section is highest when the center-of-momentum energy is somewhat above $2m_e c^2$, so one must typically assume the number of photons varies as $N_\gamma(> \nu) \propto \nu^{-\alpha}$, where $\alpha > 1$, to extrapolate from the observed photons to those that might absorb them (those with energies $\sim \Gamma^2(m_e c^2)^2/(h\nu)$, typically not observed). Our criterion for the fireball to be transparent is that $\tau_{\gamma\gamma} \leq 2/3$ for the observed photons. This requires that the Lorentz factor satisfy (Piran 1999)

$$\Gamma^{4+2\alpha} \gtrsim 1.1 \times 10^8 \left(\frac{E_\gamma}{10^{52} \text{ erg}} \right) \left(\frac{t'_{\text{obs}}}{35 \text{ s}} \right)^{-2}, \quad (69)$$

assuming the fraction of observed photon pairs with sufficient energy to pair produce is unity (an over estimate). Note, $t'_{\text{obs}} = t_{\text{obs}}/(1+z)$, where t_{obs} is the observed duration at Earth and z is the redshift of the GRB. Direct observations of the high energy (1 - 20 MeV) photons from GRB 990123 imply $\alpha \simeq 2$ (Briggs et al. 1999), and we adopt this value, as it is typical of many bursts. “No High Energy” bursts, such as GRB 980425,

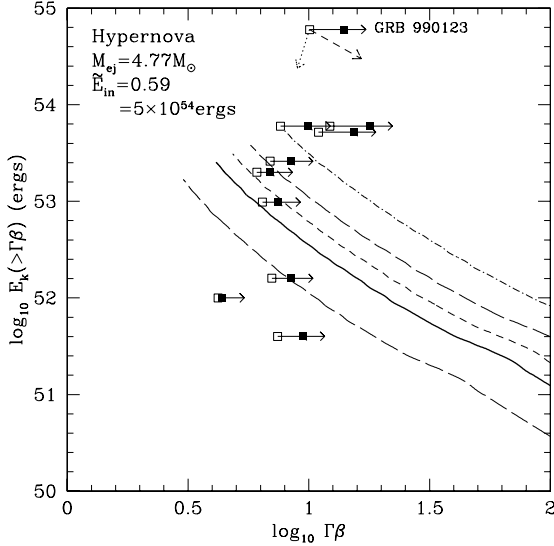


Fig. 10.— Cumulative kinetic energy distributions of ejecta from extreme hypernova explosions, modeled in our SN 1998bw progenitor. Predictions are based on the analytic approximations of §2. The fiducial model is shown by the *solid* line. The upper and lower *long-dashed* lines show the effect of increasing and reducing E_{in} by a factor of 1.5, respectively. Uncertainties in the spherical correction factor for postshock acceleration lead to $\sim 25\%$ uncertainty in the final energy distribution. The shock velocity normalization coefficient employed in these models is $A = 0.736$. However, there is some evidence from simulation that this value may increase for $\tilde{E}_{\text{in}} \sim \mathcal{O}(1)$. The fiducial model with $A = 0.8$ results in the *dashed* line. Combining these two factors, with the increased value of E_{in} results in a maximal model (*dot-dashed* line). The *squares* show the required isotropic energies $E_{\gamma}/\epsilon_{\gamma}$, with $\epsilon_{\gamma} = 0.5$, of the cosmological GRBs with detected optical afterglows, plotted at the minimum values of $\Gamma_f \beta_f$ implied by external (*solid*) and $\gamma - \gamma$ (*open*) opacity constraints (Table 3). Note that the minimum $\Gamma_f \simeq \bar{\Gamma}/2$. The *dotted arrow* shows the effect on the $\gamma - \gamma$ opacity constraint for GRB 990123 of adopting a smaller $E_{\gamma} = 1.2 \times 10^{54}$ ergs (e.g. Briggs et al. 1999), consistent within cosmological uncertainties, while the *dashed arrow* shows the effect of applying the constraint to the first major pulse of the lightcurve with FWHM ~ 10 s and energy $\sim 1/2$ of the total.

with $\alpha > 4.5$ between 100 and 300 keV (Pendleton et al. 1997), are not severely constrained by this opacity. There is some evidence for harder spectra ($\alpha \sim 1 - 1.5$), up to 100 MeV - GeV energies in a few bursts where observations are available (over the same time periods as the keV burst) (Hurley et al. 1994; Schneid et al. 1995; Dingus et al. 1997), and such hard slopes would increase the minimum Lorentz factor. The value of Γ in equation (69) ought to represent a frame in which the photon distribution is isotropic, i.e., the frame of the cooling postshock fluid; for simplicity, we shall identify this with the mean (mass-weighted) Lorentz factor of the relevant portion of the ejecta, $\bar{\Gamma}$.

In an external-shock model, the surrounding material whose presence is necessary to liberate the burst energy inevitably introduces a second source of opacity. Adopting a wind model ($\rho \propto r^{-2}$) for this material, and requiring its optical depth be less than $2/3$ (i.e., requiring $r(E_{\gamma}) = r(t'_{\text{obs}}) > R_p$ in equations [58], [59], and [62]), we find

$$\bar{\Gamma}(\bar{\Gamma} - 1)\Gamma_{\text{shell}}^4 > \frac{3E_{\gamma}f_{\text{kn}}\kappa_{\text{es}}}{32\pi\epsilon_{\gamma}t'_{\text{obs}}{}^2c^4}. \quad (70)$$

Note, $\Gamma_f \simeq \Gamma_{\text{shell}} \simeq \bar{\Gamma}(> \Gamma_f)/2$, for $n = 4$ and $\Gamma_f \gg 1$, (equation 34), and so

$$\bar{\Gamma} \gtrsim 11 \left(\frac{E_{\gamma}}{10^{52} \text{ erg}} \frac{0.5}{\epsilon_{\gamma}} \right)^{1/6} \left(\frac{t'_{\text{obs}}}{35 \text{ s}} \right)^{-1/3}, \quad (71)$$

as long as the implied $\bar{\Gamma} \gg 1$.

Often, models of GRBs or their afterglows assume a uniform rather than a wind ambient medium. In this case, the opacity of the swept-up gas is not at issue, if the burst is not in an obscured region. In an external shock model, one may constrain $\bar{\Gamma}$ by assuming a hydrogen number density n_{H} and requiring that sufficient mass be swept up to thermalize the kinetic energy of the ejecta:

$$\bar{\Gamma} \simeq 88 \left(\frac{E_{\gamma}}{10^{52} \text{ erg}} \frac{0.5}{\epsilon_{\gamma}} \right)^{1/8} \left(\frac{t'_{\text{obs}}}{35 \text{ s}} \right)^{-3/8} n_{\text{H}}^{-1/8}. \quad (72)$$

This constraint on $\bar{\Gamma}$ is less severe in more dense regions, which is why the opacity constraint is the more relevant one for wind interaction models.

In an external-shock model, t'_{obs} is the total duration of the burst, and significant substructure is difficult to explain (Sari & Piran 1997); in an

internal-shock model, t'_{obs} is the duration of an individual pulse. In either case, the total duration sets a lower limit for the Lorentz factor: we give these lower limits in Table 3, for ten bursts with known redshifts. Like GRB 980425, most of these bursts show little fine (sub-second) structure in their γ -ray light curves. The profiles are quite simple with most of the energy contained in one or two pulses lasting $\gtrsim 10$ s. Note that some substructure may be produced by the interaction of an external shock with an inhomogeneous medium (Dermer & Mitman 1999; Fenimore et al. 1999). Instabilities in accelerating shocks (Luo & Chevalier 1994) may also create variability. Strong density jumps in the progenitor may lead to variable energy release from the postshock flow as different layers crash into the decelerating region. Structure was observed in the radio emission from SN 1998bw (Kulkarni et al. 1998; Wieringa, Kulkarni, & Frail 1999), which is indubitably an external shock; the same can be said for fluctuations in other radio supernova light curves (e.g., 1979c; Weiler et al. 2000), which are attributed to variations in the ambient density.

To gauge how difficult it is for a spherical hypernova to satisfy the above constraints on energy and velocity of relativistic ejecta, we adopt an extreme explosion of $E_{\text{in}} = 5 \times 10^{54}$ erg, perhaps liberated during the formation of a $10 M_{\odot}$ black hole. We note that models for magnetic extraction of this energy on timescales short compared to the break-out time may require field strengths in excess of 10^{15} G (MacDonald et al. 1986). For lack of a better model, we surround the nascent black hole with the $\sim 5M_{\odot}$ envelope of model CO6 (§3.1). This gives $\tilde{E}_{\text{in}} \simeq 0.59$, placing the explosion in a regime untested by our simulations. Regardless, we employ our analytic approximations to investigate the expected energy distribution of the hypernova’s ejecta (Figure 10).

We compare these predictions with the required ejecta energies and minimum Lorentz factors from opacity constraints of GRBs with observed optical afterglows, listed in Table 3. Note that $\Gamma_f \simeq \bar{\Gamma}(> \Gamma_f)/2$, for $n = 4$ and $\Gamma_f \gg 1$, (equation 34). We require $E_k(> \bar{\Gamma}/2) = E_{\gamma}/\epsilon_{\gamma}$. There is a wide range of observed energies, yet quite similar minimum Lorentz factors are implied from the photon-photon and external opacity constraints, spanning a range from about 10 to 40. These

values are lower than those commonly quoted in the literature (e.g. Lithwick & Sari 2001), because the bursts in question have relatively smooth time profiles, and because our adoption of the external-shock hypothesis dictates that the age of a burst, rather than the timescale of its substructure, be used to constrain the Lorentz factor. Our extreme hypernova models can satisfy these requirements in three, and potentially six (given the uncertainties), of ten cases. However, the most energetic bursts require preferential viewing of asymmetric explosions (§2.5). Since the most luminous GRBs do not differ from typical GRBs in any significant manner except luminosity, it is therefore likely that asymmetric explosions are required for all cosmological GRBs. Nonetheless, these results demonstrate the potential importance of the trans-relativistic shock acceleration mechanism for GRB engines.

Afterglows potentially pose a difficult constraint on spherical models invoking shock acceleration and external emission, as there must be much more energy in slower ejecta than implied by the burst. We have found $E_k(> \Gamma_f \beta_f) \propto 1/(\Gamma_f \beta_f)$ (equation 36), approximately, for values of $\Gamma_f \beta_f$ significantly above $1 + \tilde{E}_{\text{in}}$; the energy rises even more sharply for low values of $\Gamma_f \beta_f$ (Figure 6). As the emitting region is continuously “refreshed” as it decelerates by this increasing source of energy (Rees & Mészáros 1998; Sari & Mészáros 2000), afterglows should evince these even higher energies. This is especially true if the emitting shell makes a transition from radiative to adiabatic dynamics between the burst and its afterglow. Freedman & Waxman (1999) argue that afterglow observations indicate an energy comparable (within a factor of three) to the energy emitted in γ -rays, despite an assumed deceleration from $\Gamma \gtrsim 100$ to $\Gamma \simeq 10$. Moreover, the emitted γ -ray energy places a lower limit on the energy content (per solid angle) of the emitting gas in its early phase.

We use the results of Sari & Mészáros (2000) to evaluate the severity of such afterglow constraints. Assuming a wind ambient medium $\rho \propto r^{-2}$ and ultrarelativistic ejecta from an envelope with polytropic index n , equation (34) and equation (3) of Sari & Mészáros gives a swept-up kinetic energy

that varies as

$$E_k \propto t_{\text{obs}}'^{(2.7+n)/(2.7+7.7n)}, \quad (73)$$

i.e., $E_k \propto t_{\text{obs}}'^{(0.2,0.17,0.13)}$ for $n = (4, 7, \infty)$. The increase in kinetic energy from 35 seconds to ten days is thus a factor of $\sim (7.6, 5.6, 3.7)$ in a model involving a hypernova and its wind, for these three values of n . Considering the uncertainties in the Freedman & Waxman results, we conclude that it cannot yet be argued that afterglow calorimetry rules out approximately spherical hypernovae as the origins of some cosmological GRBs, especially those with relatively low E_γ for which Freedman & Waxman find the afterglow to be about three times more energetic than the GRB.

All of the above constraints are somewhat assuaged if the progenitor or its explosion are asymmetric. As discussed in §2.5, an assessment of the implications of asymmetrical explosions requires that multidimensional simulations be interpreted using our equation (54). Under the admittedly simplistic sector approximation, we found that relatively small variations in the energy per unit mass of the ejecta can have substantial effects on the energy of the resulting relativistic ejecta. More accurately, given a shock intensity p below a given column density on some patch of the stellar surface, the kinetic energy in that direction (above some chosen velocity) varies as $p^{5.35\gamma_p}$. For $n = (4, 7)$, the shock intensity p need only be enhanced a factor (1.99, 2.12) at some reference column to increase the kinetic energy in that direction by a factor of one hundred, at all velocities for which the ejecta experienced an accelerating shock. This enhancement would be enough to bring even GRB 990123 within the reach of hypernova models. We eagerly await simulations that will evaluate whether this degree of asymmetry is realistic.

In summary, while our ad hoc and extreme spherical hypernova model is consistent with many of the GRBs with observed afterglows, it appears likely that the most energetic bursts require asymmetric progenitors or energy injection. Given this possibility, trans-relativistic blast waves from hypernovae may in principle account for the energetics and ejecta velocities of cosmological bursts, though it is too early to decide if this mechanism is primarily responsible for their origin. The association of these cosmic GRBs with the stellar

population of their host galaxies (Bloom et al. 2000b), and more tentatively with star forming regions (Kulkarni et al. 2000; Djorgovski, Bloom, & Kulkarni 2000; Galama & Wijers 2000), argues in favor of a connection with the deaths of massive stars and against scenarios involving neutron star mergers. The difficulty of avoiding baryon loading while trying to escape the stellar progenitor, encountered even in highly asymmetric jet models (Aloy et al. 2000), is overcome in the hydrodynamic shock acceleration mechanism. The efficiency of γ -ray production is higher for a blast wave producing these photons from both external and internal shocks, compared to one that radiates solely via internal shocks (Kumar 1999). While external shocks are inefficient at producing substructure (Sari & Piran 1997), the lightcurves of the bursts with observed afterglows are relatively smooth, with little power in sub-second features. It remains to be demonstrated if our model can account for moderate variability, perhaps via the interaction with circumstellar inhomogeneities (Dermer & Mitman 1999; Fenimore et al. 1999) or via the production of postshock velocity perturbations by the growth of instabilities in the accelerating shock (Luo & Chevalier 1994) or by the presence of steep density shelves in the progenitor's atmosphere. Further investigation is also required to determine whether a model with monotonically decelerating forward and reverse shocks produces spectra (see Sari & Mészáros 2000) that resemble those of cosmological GRBs as well as their afterglows.

3.3. Ejecta from Compact Objects

3.3.1. White Dwarfs

Accreting white dwarfs near the Chandrasekhar mass face two quite distinct fates. Type Ia supernovae involve the release of $\sim 10^{51}$ ergs in $1.4 M_\odot$ ($\tilde{E}_{\text{in}} \sim 4 \times 10^{-4}$), in either a deflagration or a detonation (Woosley & Weaver 1986). Approximating a detonation as an adiabatic point explosion, equation (37) with $f_\rho = 0.3$, $n = 1.9$, and $A = 0.705$ (values derived from a model provided by Lee Lindblom) gives $E_k(\Gamma_f > 3, 10) = (35, 1.1) \times 10^{39}$ ergs, respectively (see also Berezhinsky et al. 1996, who presented an approximate treatment of shock and postshock acceleration in WDs). These energies are too small to produce

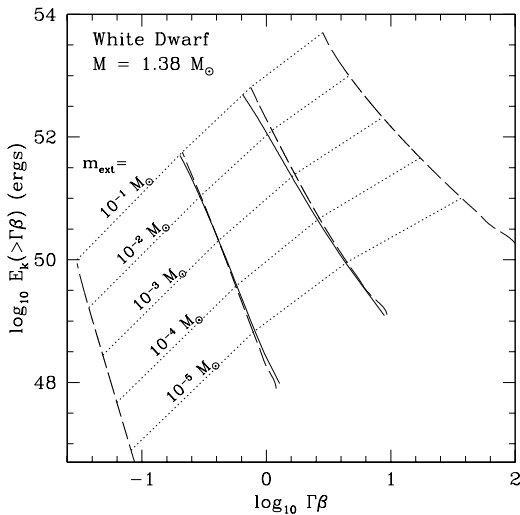


Fig. 11.— Kinetic energy distribution with velocity for the outer $0.1 M_{\odot}$ of ejecta from white dwarf explosions. Numerical simulation results are shown by the *solid* lines, and analytic predictions from §2, integrated over the progenitor density distribution, by the *long dashed* lines. The agreement is excellent for the outermost ejecta, but, as expected, deviates towards the interior, where approximations of the analytic theory break down. Models of AIC (Fryer et al. 1999) tend to place $\sim 10^{50}$ ergs in $0.01 - 0.1 M_{\odot}$.

observable GRBs.

Another possible outcome, if the central density is high enough to allow electron capture prior to carbon or neon ignition, is accretion-induced collapse (AIC) from white dwarf to neutron star (e.g., Woosley & Baron 1992; Fryer et al. 1999, and references therein). Such events resemble the core-collapse supernovae of massive stars, but lack the ram pressure and long timescale introduced by an extended infalling envelope. Goodman et al. (1987) suggested that neutrino annihilations above the neutrinosphere of a newly-formed neutron star could vent $\sim 0.3\%$ of the neutrino luminosity into the nearby volume; if this region were baryon-free, a relativistic wind of energy $\sim 10^{50}$ erg would result, which could drive a GRB (Dar et al. 1992). However, the neutrinosphere underlies a massive layer of baryons (Woosley & Baron 1992), so there results instead a neutrino-driven wind of velocity $\sim c/3$. This may either expel an exterior envelope, or expand freely if there is no envelope left (Fryer et al. 1999). There is not sufficient energy in such winds to power the cosmological GRBs listed in Table 3, and moreover they cannot satisfy the Lorentz factor constraint, (69) or (71). They could only produce fast ejecta through shock acceleration; but, since the mean velocity of the ejecta cannot exceed $c/3$ (§2.6.1), only a small fraction of the energy is available at appreciable Γ_f .

In addition to the energy injection from this wind, there is also a prompt shock from the core collapse (which stalls; Fryer et al. 1999), and “delayed” heating by neutrino absorption behind the stalled shock; the latter drives ejection in the model of Fryer et al.. This simulation has $\sim 10^{50}$ ergs deposited in $\sim 0.1 M_{\odot}$, for a mean expansion velocity of $\sim c/30$. Equation (55) would predict this total energy for $R \sim 1500$ km. In the calculation, (20%, 60%, 90%) of the ejected mass fell below (200, 300, 400) km before being ejected (C. Fryer, 2000, personal communication). This indicates that the theory of §2.6, which neglects infall motions and assumes ejection from a thin outer layer, is not directly comparable to these AIC models.

Because the total energies are too low and the typical expansion velocities too slow, Woosley & Baron (1992) and Fryer et al. (1999) conclude that AICs do not cause cosmological GRBs like those

listed in Table 3. Although this is a valid conclusion, for completeness we investigate the relativistic ejecta from these events, including cases of more extreme energy release than predicted by Fryer et al. (1999).

Our $1.38 M_{\odot}$ progenitor model, from Lindblom (1999), uses for its equation of state a fully degenerate, non-interacting Fermi gas. The initial density distribution is shown in Figure 7. We note this model has a radius twice that of the WD considered by Fryer et al. (1999).

Figure 11 shows $E_k(> \Gamma\beta)$ vs $\Gamma\beta$ for explosions of different energies in our WD progenitor. As these simulations neglect gravity and the initial collapse motion of the progenitor, they should be considered rough approximations to the result. The lowest curve in this figure matches the mass and energy of the Fryer et al. simulations; higher curves address hypothetical cases with much higher energies. Although an asymmetrical explosion, which may be expected in the collapse of a rapidly rotating object, might enhance the energy along the line of sight, we concur with Woosley & Baron (1992) and Fryer et al. (1999) that AICs do not make cosmological GRBs. We are not in a position to judge whether magnetized winds or jets from such events (Shaviv & Dar 1995) produce GRBs.

3.3.2. Neutron Stars

Explosions in neutron stars (NSs) powered by a phase transition to a “strange” star have been considered as a potential GRB mechanism (Fryer & Woosley 1998, and references therein). Fryer & Woosley simulated the collapse and bounce resulting from a neutron star phase transition to derive properties of the ejecta. These were then used to implement higher resolution simulations of shock propagation in the outer 0.01 - $0.001 M_{\odot}$, with resolution down to $10^{-11} M_{\odot}$. This latter stage made use of a nonrelativistic code, with a simple approximation based on energy conservation to derive upper limits on the kinetic energy distribution at high (> 40) Lorentz factors. However, this approximation neglects the concentration of energy in the outermost ejecta at the expense of the inner, due to pressure gradients in the flow (see §2.2).

Fryer & Woosley’s most energetic explosion involved $0.017 M_{\odot}$ ejected with $\sim 5 \times 10^{51}$ ergs from

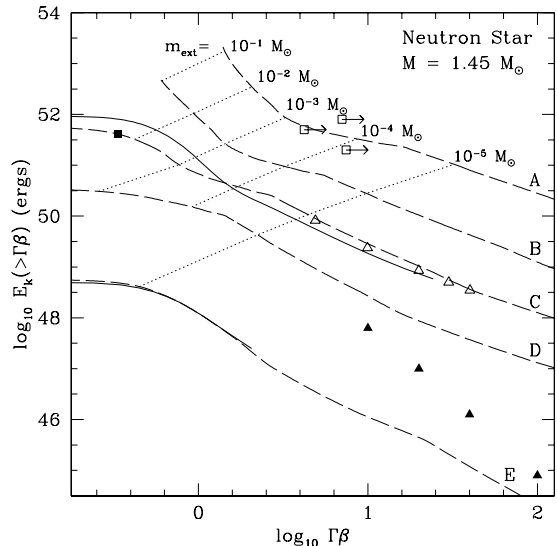


Fig. 12.— Kinetic energy distribution with velocity for ejecta from neutron star explosions, after subtracting off the initial gravitational binding energy. Results for two simulations are shown (*solid lines*), and compared to analytic predictions from §2, integrated over the progenitor density distribution (*long dashed lines*). The analytic predictions amplify the dependence of velocities resulting from abrupt changes in the initial density distribution compared to simulation, which can more accurately handle these effects. The analytic predictions are used to further explore the parameter space. Model C, in which ejecta of mass $0.017 M_{\odot}$ carry away 4×10^{51} ergs of kinetic energy (*solid square*) is closest to the energetic model of Fryer & Woosley (1998). The *solid triangles* are Fryer & Woosley’s predicted upper limits from nonrelativistic shock propagation models, including a relativistic correction. Our estimates, including the direct energy approximation of equation (57b) (*open triangles*) are about two orders of magnitude higher. The dotted lines show mass contours. These reveal the greater ejecta masses that result from the explosions of higher energy. The *open squares* show the $\gamma - \gamma$ opacity constraint of the three weakest cosmological GRBs from Table 3.

a neutron star of initial mass $1.4 M_{\odot}$. Using the Gnatyk shock formula (eq. 8) and their simple estimate of postshock acceleration, they inferred an upper limit of 10^{46} ergs for material traveling with $\Gamma_f > 40$, and concluded that NS phase transitions cannot power cosmological GRBs. However, as these events are sufficiently energetic to explain some of these bursts, and as the mean velocity implied by their ejecta is $\sim 0.51c$ (i.e., $\bar{\Gamma} \simeq 1.16$), we wish to revisit this issue with our improved treatment of the dynamics.

As the injected energy is small compared to the binding energy of the NS envelope, and as only a small fraction of this envelope is blown away, the results of §2.6 apply. In the simulation of Fryer & Woosley (1998), the stellar surface is shocked after it has fallen from 11 km to 10 km. We use the low-density Harrison-Wheeler (HW) equation of state (Glendenning 1997) to obtain the appropriate value of n underneath $0.017 M_{\odot}$ of material: the pressure at this depth is 5×10^{32} dyne cm^{-2} , so we adopt the value $n \simeq 12$ appropriate for the highest pressure listed (10^{31} dyne cm^{-2}). Using these parameters, equation (55) predicts a final kinetic energy of 3.3×10^{51} erg, sufficiently close to the value ($\sim 5 \times 10^{51}$ erg) quoted by Fryer & Woosley (1998) to give us faith in our approximations. As an added check, note that Fryer & Woosley consider a weak explosion that ejects $10^{-3} M_{\odot}$ with $\sim 3 \times 10^{50}$ erg; equation (55) predicts 2.0×10^{50} erg for this ejecta mass. Thus, we see that the theory of §2.6 underestimates the kinetic energy in the simulations by $\sim 50\%$. This is not due to our approximation of Newtonian gravity, as Fryer & Woosley’s calculations were also Newtonian, but may be due to our neglect of in-fall of the outer layers, before they are shocked, or their neglect of special relativity.

We apply equation (57b) to predict the kinetic energy in ejecta at some higher Lorentz factor. Note a value of $n = 4$, appropriate for the outer distribution, is used in evaluating $F(\Gamma_f \beta_f)$, while $n = 12$, appropriate for the base of the ejecta, is used to evaluate the preceding terms that normalize the distribution. Taking $f_{\text{sph}} = 0.85$, we obtain kinetic energies of $(8.2, 2.4, 0.85, 0.45, 0.35) \times 10^{49}$ ergs for $\Gamma_f > (5, 10, 20, 30, 40)$; presumably, these energies should be increased by $\sim 50\%$ to account for the discrepancy noted above. This gives an estimate of $\sim 0.52 \times 10^{49}$ erg in material with

$\Gamma_f > 40$, more than two orders of magnitude greater than Fryer & Woosley’s inferred upper limit.

We validate this result with direct simulation of relativistic explosions in a neutron star progenitor, constructed using the Harrison-Wheeler equation of state at low densities (Glendenning 1997) and with the pressure extrapolated to higher densities with a polytrope, using Newtonian gravity. The central pressure and polytropic index were varied to reproduce a realistic mass and radius. The initial density distribution is shown in Figure 7. Our method follows that employed for explosions in white dwarfs, except now it is necessary to account for the progenitor’s gravity (§2.6). We make a first order correction to our non-gravitating simulations by subtracting off the initial gravitational binding energy of ejecta from their final energy distribution. In Figure 12 we compare simulation results with our analytic approximations to the shock dynamics, applied to the progenitor density distribution, again accounting for the gravitational binding energy. We also show (*open triangles*) the direct energy approximation (equation 57b), without the calibration correction to Fryer & Woosley results, which acts to increase the energies. Our different methods are in good agreement, and are larger than Fryer & Woosley’s estimate (*solid triangles*) by between two and three orders of magnitude, a fact which highlights the importance of a correct treatment of postshock acceleration.

For a uniform ambient density of density $n_H \sim 1 \text{ cm}^{-3}$, equation (72) indicates that $\Gamma_f \simeq \bar{\Gamma}/2 \gtrsim 44$ if a GRB with $E_{\gamma} = 10^{52}$ ergs is to last ~ 35 s in its rest frame, although lower values of Γ_f may be acceptable if the burst occurs in the dense circumstellar environment of a companion. The photon-photon opacity constraint, eq. (69), requires $\Gamma_f \simeq \bar{\Gamma}/2 \gtrsim 5$ for such a burst, if the photon index is $\alpha = 2$.

Considering the cosmological GRBs listed in Table 3, we see that neutron-star phase transitions can match the energies of several such bursts (970778, 970508, and 000301C) if Lorentz factor constraints are ignored. However, the required Lorentz factors seem to be about $\Gamma_f \gtrsim 5 - 10$ for the slowest part of the ejecta, if in a sufficiently dense environment. The kinetic energy of such ejecta is only a few percent of the total, about

10^{50} ergs. These considerations argue against NS phase transitions as the origins of cosmological GRBs, unless the ejected mass has been significantly underestimated or the energy can be collimated.

4. Conclusions

Any viable model for the central engines of gamma-ray bursts, especially for those bursts known to be at cosmological distances, must explain the existence of large energies (10^{51-54} erg, if isotropic) in ejecta moving sufficiently fast that, when converted into radiation, it escapes as non-thermal radiation. Such velocities require very little “baryon loading,” a constraint that many theories for gamma-ray burst central engines address. In this paper, we have investigated the possibility that shock hydrodynamical acceleration, first proposed as a source of GRBs by Colgate (1974), may concentrate sufficient energy in the fastest ejecta to satisfy this constraint. We consider ordinary and over-energetic supernova explosions, making specific models for the hypothesized class of supernova gamma-ray bursts (S-GRBs; Bloom et al. 1998a) whose existence was suggested by SN 1998bw and GRB 980425. We also calculate the yield of relativistic ejecta from hypothetical models for extraordinary “hypernova” explosions, as well as possible accretion-induced collapses of white dwarfs and sudden condensations of neutron stars.

As an exemplary case, we have considered in detail (§3.1) specific models for supernova 1998bw and the gamma-ray burst (GRB 980425) that it may have produced, considering the constraints of the GRB and the supernova’s early radio emission in the context of progenitor models constructed (by Woosley et al. 1999) to fit its light curve. One goal of this investigation has been to evaluate assertions (Wang & Wheeler 1998; Woosley et al. 1999; Höflich et al. 1999) that spherical models for this explosion cannot explain the GRB. After properly accounting for the the trans-relativistic shock and postshock dynamics as well as the interaction with a surrounding stellar wind, we are able to account for all of the observations of this event with a spherical energetic Type Ic supernova from a progenitor with high ($\sim \text{few} \times 10^{-4} M_{\odot} \text{ yr}^{-1}$) mass loss rate, consistent with observed carbon-

rich (WC) Wolf-Rayet stars. Our conclusion that the fastest ejecta need not be asymmetric is reminiscent of the fact that the radio shell around SN 1993J was spherical (Marcaide et al. 1997) despite the assertion (Höflich et al. 1996) that its polarization implied an asymmetrical explosion. Our model for SN 1998bw and GRB 980425 invokes a circumstellar environment similar to that inferred around SN 1997cy, which may be associated with GRB 970514 (Turatto et al. 2000); however the two-second duration of this burst may be difficult to reconcile with the external shock hypothesis.

In order to quantify the process of relativistic mass ejection, we have extended the nonrelativistic theory of supernova explosions (Matzner & McKee 1999) into the relativistic regime. Finding that the energetics of such ejecta depend sensitively on the velocity of the shock front as it emerges from the stellar surface, we present in §2.1 a formula for this velocity (eqs. [14] and [15]) that handles the transition from nonrelativistic to relativistic flow more accurately than does the prediction of Gnatyk (1985) (equation 8). Whereas for Matzner & McKee (1999) it sufficed to take a universal value for the normalization of the shock velocity (and also applied an overall energy conservation constraint to their ejecta-density models), we have found it necessary to present (eqs. [4], [5], and [6]) a refined estimate for this coefficient – one that responds to the initial density distribution of the progenitor.

The motivation for such precision is the sensitive dependence of the final velocity of a mass element on the velocity of the shock that struck it: in the relativistic, planar limit this is $\Gamma_f \propto \Gamma_s^{2.7}$. This postshock acceleration, neglected in many works that invoke shock acceleration, is crucial for the production of appreciable energy in fast ejecta. In §2.2 we present formulae for this postshock acceleration in the planar limit (eq. [17]) and for the effect of spherical geometry to reduce the acceleration (eqs. [20] and [21]). The latter is somewhat uncertain, due to the limitations of our numerical calculations; however, since this correction is a factor of order unity, the energetics of relativistic ejecta are not especially sensitive to it. Because we account properly for postshock acceleration, our predictions for the energetics of relativistic ejecta are much larger than presented in previous works that considered hydrodynamical

shock acceleration in the context of supernovae, accretion-induced collapses of white dwarfs, and phase transitions in neutron stars.

With the dynamics of trans-relativistic mass ejection well in hand, we turned in §2.3 to an evaluation of the amount of kinetic energy expected in ejecta traveling above some given lower limit. Equation (37) represents an accurate approximation for this kinetic energy distribution under the assumption that the outer stellar density distribution is that of a polytropic atmosphere of index n . This formula shows that the kinetic energy distribution rolls over quite slowly (fig. 6) from $E_k \propto \beta_f^{-(3.35+5.35/n)}$, to $E_k \propto \Gamma_f^{-(0.58+1.58/n)}$, as the final velocity in question goes from nonrelativistic ($\Gamma_f \beta_f \ll 1$) to relativistic ($\Gamma_f \beta_f \gg 1$); this slow limiting behavior comes from fact that relativistic final velocities originate from only mildly relativistic shocks. For typical values of n , the kinetic energy in relativistic ejecta decreases as $\sim 1/\Gamma_f$; this gentle decline with velocity allows for significant energy at relatively high Γ_f .

We next developed (§2.4) a theory to assess what characteristics of a stellar envelope make it especially efficient at converting a given dose of injected energy into relativistic motion – the astrophysical analog of how to design a good bullwhip. If the envelope mass is fixed, we found that more centrally-condensed envelopes are more efficient producers of high-velocity ejecta. If instead the progenitor star is given, then the energy in fast ejecta is enhanced by allowing as much of it as possible to collapse (minimizing M_{ej}), as this increases the energy per mass of what escapes.

Evaluating the energetics of relativistic ejecta for radiative stellar progenitors in §2.4, we derived expressions appropriate for regions dominated by electron scattering (eq. [47]) or bound-free or free-free (eq. [49]) absorption, assuming different possible compositions for the outer envelope. For the Thomson opacity case, the central concentration of the atmosphere – and therefore its efficacy at producing relativistic ejecta – is enhanced if the stellar luminosity approaches the Eddington limit.

It should be kept in mind that typical supernovae in supergiant stars are not capable of creating any relativistic ejecta (Matzner & McKee 1999), because there, shock acceleration ends at nonrelativistic velocities at a depth that matches

the width of the shock. In this paper, we have only considered progenitors sufficiently compact and exploding with enough energy, that relativistic ejection does occur.

Although we do not model asymmetrical explosions, our theory for shock and postshock dynamics can be applied to simulations of such an event. In §2.5 we present a formula (eq. [54]) for the relativistic yield of each patch of the stellar surface, in terms of the intensity of the (nonrelativistic) shock as it might be observed in such a simulation. As multidimensional simulations cannot yet afford to treat relativistic dynamics with the extremely fine zoning that would be required to match the predictive power of this formula, it could be quite useful in future investigations.

In §2.6 we have put our dynamical formulae to another use: the prediction of what will be ejected in the case of an explosion so weak that it only ejects a small mass from the outside of the star. Assuming ballistic motion after a brief phase of acceleration, the escape velocity marks the inner boundary of the ejecta. For this reason, the overall kinetic energy (eq. [55]) and the kinetic energy above some given velocity (eqs. [56], [57a], and [57b]) are proportional the initial binding energy of the ejecta. Applied to neutron star phase transitions in §3.3.2, equation (55) predicts within 50% the average kinetic energy per gram in the ejecta in Fryer & Woosley (1998)’s simulations. These considerations also provide some insight into the characteristic shock velocity at the base of the ejecta (§2.6.1).

After calculating in §3.1.1 the energy distribution of relativistic ejecta from Woosley et al. (1999)’s model CO6 for SN 1998bw, and demonstrating that this can explain both the observed gamma-ray burst (~ 35 s timescale; §3.1.2) and the rapidly expanding radio shell (~ 12 day timescale; §3.1.3), we turned to the modeling of far more energetic “hypernova” explosions in §3.2. The association of GRB afterglows with the stellar population of their host galaxies (Bloom et al. 2000b), and more tentatively with star forming regions (Kulkarni et al. 2000; Djorgovski, Bloom, & Kulkarni 2000; Galama & Wijers 2000), argues in favor of a connection with the deaths of massive stars and against scenarios involving neutron star mergers. Furthermore, the difficulty of avoiding baryon loading while trying to escape the stellar

progenitor, encountered even in highly asymmetric jet models (Aloy et al. 2000), is overcome in the hydrodynamic shock acceleration mechanism.

In this model GRBs, like their afterglows, would represent radiation from an external shock that accelerates the ambient medium, with an extra component (of comparable luminosity) from the reverse shock that decelerates the ejecta; both shocks must decelerate monotonically. Note that the higher efficiency of γ -ray production in models including external shocks, compared to those based solely on internal shocks (Kumar 1999), gives external shock models less stringent total energy requirements. The spectral signature of such two-shock structures (Sari & Mészáros 2000) should be used to test this hypothesis; however, the reverse shock is buried under more material (by a factor of Γ) and may not be visible early on. While highly structured GRB profiles are difficult to accommodate in this scenario (Sari & Piran 1997), most of the GRBs with afterglows have relatively smooth pulses. Small amounts of substructure may result from interaction with an inhomogeneous medium (Dermer & Mitman 1999; Fenimore et al. 1999), or from postshock velocity perturbations produced by instabilities in the accelerating shock (Luo & Chevalier 1994) or the presence of steep density shelves in the progenitor’s atmosphere. More detailed modeling of these processes is required. In some bursts, there is evidence that a smooth and soft component of the GRB flux is an early manifestation of the afterglow (Burenin et al. 1999; Giblin et al. 1999; Burenin 2000; Tkachenko et al. 2000). The existence of this component agrees with the external-shock model, although the fact that it does not account for the entire GRB does not. GRB 990123 had an optical flash that has been interpreted (e.g., Sari & Mészáros 2000) to arise from reverse-shock emission; however, this model invoked a brief rather than a continuous collision of ejecta with the swept-up shell.

Because an external medium is necessary to liberate the energy, the Lorentz factor of the emitting region must not only exceed the usual lower limit from photon-photon opacity (eq. [69]), but also a limit due to the opacity of a circumstellar wind (eq. [71]) or the density of a uniform background (eq. [72]). The observed gamma-ray energies thus become, in a spherical model for the burst, lower

limits for the amount of energy in ejecta whose Lorentz factor satisfies these constraints. As the bursts in question have quite smooth time profiles, and because our adoption of the external-shock hypothesis dictates that the age of a burst, rather than the timescale of its substructure, be used to constrain the Lorentz factor, we predict smaller minimum Lorentz factors than commonly quoted in the literature, by factors of ten or more. This eases the baryon-loading constraint by a similar amount.

We find that a simple, and admittedly extreme, spherical hypernova model satisfies the energy and velocity constraints of many of the observed cosmological GRBs. The most energetic bursts, such as GRB 990123, require asymmetric explosions. These need not be highly aspherical as the results of §2.5 show that a mild (factor of two) variation in shock intensity at a given column below the surface of the star can lead to an extreme (factor of 100) variation in the observed burst intensity. If such variations are justified by simulations, this result may allow even the most energetic bursts to be explained by hydrodynamical shock acceleration in aspherical hypernovae. Since the very luminous bursts do not differ from typical ones in any significant manner other than luminosity, it is likely that all cosmological bursts are aspherical, and as a result there is no need to invoke hypernova models as extreme as the one we have considered.

Since we predict a kinetic energy that decreases with Lorentz factor roughly as $1/\Gamma_f$, there must be more energy in slower relativistic ejecta, and (if $E_{\text{in}} \ll M_{\text{ej}}c^2$) much more in nonrelativistic ejecta as well. As the shocked region decelerates, an increasing fraction of this energy should appear in the afterglow; therefore, estimates of afterglow energetics (e.g., Freedman & Waxman 1999) may potentially rule out such models in the future. However, having demonstrated in equation (73) that the energy of the shocked shell increases quite slowly, we find that Freedman & Waxman’s constraints cannot yet rule out hypernovae as sources of cosmological GRBs.

Energetic events in compact objects have also been considered as engines for GRBs. White dwarfs (§3.3.1) explode as type Ia supernovae, but the relativistic ejecta from SNe Ia are too weak to be of much interest. Accretion-induced col-

lapse of white dwarfs can potentially concentrate a somewhat smaller energy ($\sim 10^{50}$ erg) in a smaller ($\sim 0.1 M_{\odot}$) mass of ejecta. Considering the simulations of Fryer et al. (1999), we predict a much greater yield of relativistic ejecta than their estimates; but not enough to power cosmological GRBs.

Neutron star phase transitions, considered in §3.3.2, are well described by the weak explosion theory of §2.6. As equation (55) gives the overall energetics of the explosion to within 50%, we are justified in using equation (56) to predict the energetics of fast ejecta. Our estimates, validated with numerical simulation, are several orders of magnitude higher than those of Fryer & Woosley (1998), who underestimated postshock acceleration. However, we note that such events do not put enough energy at sufficient Lorentz factor to satisfy the observational constraints for distant bursts with afterglows.

We thank Stan Woosley and Lee Lindblom for kindly providing models of SN 1998bw's progenitor star and a white dwarf, respectively. We also thank M. Aloy, A. Filippenko, Z.-Y. Li and the referee for detailed comments on the manuscript. We are grateful to A. Cumming, R. Fisher, P. Kumar, A. MacFadyen, R. Sari, E. Scannapieco, N. Shaviv, and A. Youdin for helpful discussions. CDM appreciates the gracious hospitality of Sterl Phinney and Roger Blandford during his visits to Caltech, as well as financial support from NSERC. The research of JCT and CFM is supported by NSF grant AST 95-30480.

REFERENCES

- Aloy, M. A., Müller, E., Ibanez, J. M., Martí, J. M., & MacFadyen, A. 2000, *ApJ*, 531, L122
- Bailyn, C. D., Jain, R. K., Coppi, P. & Orosz, J. A. 1998, *ApJ*, 499, 367
- Baring, M. G. and Harding, A. K. 1997, *ApJ*, 491, 663
- Berezinsky, V. S., Blasi, P., & Hnatyk, B. I. 1996, *ApJ*, 469, 311
- Blandford, R. D., & McKee, C. F. 1976, *Phys. of Fluids*, 19, 113
- Bloom, J. S. et al. 1998a, *ApJ*, 506, L105
- Bloom, J. S. et al. 1998b, *ApJ*, 508, L21
- Bloom, J. S. et al. 1999, *Nature*, 401, 453
- Bloom, J. S. et al. 2000, *GCN* 661
- Bloom, J. S., Kulkarni, S. R., & Djorgovski, S. G. 2000, *astro-ph/0010176*
- Briggs, M. S. et al. 1999, *ApJ*, 524, 82
- Burenin, R. A. et al. 1999, *A&AS*, 138, 443
- Burenin, R. A. 2000, *Astronomy Letters*, 26, 269
- Burrows, A. 1987, *ApJ*, 318, L57
- Castro, S. M. et al. 2000, *GCN* 605
- Centrella, J. M. 1986, in *Dynamical Spacetimes & Numerical Relativity*, ed. Joan M. Centrella (Cambridge), 326
- Chandrasekhar, S. 1939, *An Introduction to the Theory of Stellar Structure* (New York: Dover)
- Chevalier, R. A. 1982, *ApJ*, 258, 790
- Chevalier, R. A. 1990, *ApJ*, 359, 463
- Chevalier, R. A., & Soker, N. 1989, *ApJ*, 341, 867
- Clayton, D. D. 1983, *Principles of Stellar Evolution & Nucleosynthesis*, Chicago
- Colgate, S. A. 1974, *ApJ*, 187, 333
- Costa, E. & Feroci, M. 1997, *IAUC* 6572
- Costa, E., Feroci, M., Piro, L., Soffitta, P., Amati, M., & Cinti, M. N. 1997, *IAUC* 6649
- Dadina, M. et al. 1999, *IAUC* 7160
- Dar, A., Kozlovsky, B., Nussinov, S., & Ramaty, R. 1992, *ApJ*, 388, 164
- Dermer, C. D., & Mitman, K. E., 1999, *ApJ*, 513, L5
- Dingus, B. L. et al. 1997, *Gamma-Ray Bursts: 4th Huntsville Symposium*, eds. Charles A. Meegan, Robert D. Preece & Thomas M. Koshut. Woodbury, New York : AIP 428

- Djorgovski, S. G., Kulkarni, S. R., & Bloom, J. S. 1999, *GCN* 289
- Djorgovski, S. G. et al. 1999, *GCN* 481
- Djorgovski, S. G., Bloom, J. S., & Kulkarni, S. R. 2000, *ApJ*, submitted (astro-ph/0008029)
- Esin, A. A. & Blanford, R. D. 2000, *ApJ*, 534, L151
- Fenimore, E. E., Cooper, C., Ramirez-Ruiz, E., Sumner, M. C., Yoshida, A., & Namiki, M. 1999, *ApJ*, 512, 683
- Feroci, M. et al. 1999, *IAUC* 7095
- Freedman, D. & Waxman, E. 2000, *ApJ*, submitted, astro-ph/9912214
- Fruchter, A. S. et al. 1999, *ApJ*, 516, 683
- Fryer, C., & Woosley, S. E. *ApJ*, 501, 780
- Fryer, C., Benz, W., Herant, M., & Colgate, S. A. *ApJ*, 516, 892
- Fynbo, J. P. U. et al. 2000, *GCN* 807
- Galama, T. J. et al. 1998, *Nature*, 395, 670
- Galama, T. J. et al. 2000, *ApJ*, 536, 185
- Galama, T. J., & Wijers, R. A. M. J. 2000, *ApJ*, submitted
- Germany, L. M. et al., 2000, *ApJ*, 533, 320
- Giblin, T. W., van Paradijs, J., Kouveliotou, C., Connaughton, V., Wijers, R. A. M. J., Briggs, M. S., Preece, R. D. & Fishman, G. J. 1999, *ApJ*, 524, L47
- Glendenning, N. K. 1997, *Compact Stars* (Springer, New York)
- Gnatyk, B. I. 1985, *Sov. Astron. Lett.* 11(5), 331
- Goodman, J., Dar, A., & Nussinov, S. 1987, *ApJ*, 314, L51
- Hamann, W.-R., Koesterke, L., & Wessolowski, U. 1995, *A&A*, 299, 151
- Harpaz, A. 1994, *Stellar Evolution*, Peters.
- Harrison, F. A. et al. 1999, *ApJ*, 523, L121
- Heger, A., & Langer, N. 1996, *A&A*, 315, 421
- Heise, J. & in 't Zand, J. 1997, *IAUC* 6787
- Höflich, P., Wheeler, J. C., & Wang, L. 1999, *ApJ*, 521, 179
- Höflich, P., Wheeler, J. C., Hines, D. C. & Trammell, S. R. 1996, *ApJ*, 459, 307
- Hogg, D. W. & Fruchter, A. S. 1999, *ApJ*, 520, 54
- Hurley, K. et al. 1994, *Nature*, 372, 652
- Hurley, K. & Cline, T. 1999, *GCN* 450
- Hurley, K., Cline, T., & Mazets, E. 2000, *GCN* 642
- Hurley, K., Mazets, E., Golenetskii, S., & Cline, T. 2000, *GCN* 801
- Iwamoto, K. et al. 1998, *Nature*, 395, 672
- Johnson, M. H., & McKee, C. F. 1971, *PRD*, 3, 858
- Kazhdan, Y. M., & Murzina, M. 1992, *ApJ*, 400, 192
- Khokhlov, A. M., Höflich, P. A., Oran, E. S., Wheeler, J. C., Wang, L. & Chtchelkanova, A. Y. 1999, *ApJ*, 524, L107
- Koesterke, L., & Hamann, W. -R. 1995, *å*, 299, 503
- Krolik, J. H. and Pier, E. A. 1991, *ApJ*, 373, 277
- Kulkarni, S. R. et al. 1998, *Nature*, 395, 663
- Kulkarni, S. R. et al. 1999, *Nature*, 398, 389
- Kulkarni, S. R. et al. 2000, in *Gamma-Ray Bursts: 5th Huntsville Symposium*, astro-ph/0002168
- Kumar, P. 1999, *ApJ*, 523, L113
- Li, Z. Y., & Chevalier, R. A. 1999, *ApJ*, 526, 716
- Lindblom, 1999, *Phys. Rev. D*, 60, 064007
- Lithwick, Y., & Sari, R. 2001, *ApJ*, submitted, astro-ph/0011508
- Litvinova, I. Y. & Nadëzhin, D. K. 1990, *Soviet Astron. Lett.*, 16 29
- Luo, D. & Chevalier, R. A. 1994, *ApJ*, 435, 815
- MacDonald, D. A., Thorne, K. S., Price, R. H., & Zhang, X.-H. 1986, in *Black Holes, the Membrane Paradigm*, ed. K. S. Thorne, R. H. Price, & D. A. MacDonald (New Haven: Yale Univ. Press)
- MacFadyen, A., & Woosley, S. E. 1999, *ApJ*, 524, 262
- MacFadyen, A., Woosley, S. E., & Heger, A. 2000, *ApJ*, submitted, astro-ph/9910034
- Marcaide, J. M. and 15 colleagues 1997, *ApJ*, 486, L31
- Martí, J. M., & Müller, E. 1994, *J. Fluid Mech.*, 258, 317
- Matzner, C. D., & McKee, C. F. 1999, *ApJ*, 510, 379
- Mészáros, P. & Rees, M. J. 1993, *ApJ*, 405, 278
- Mészáros, P. 1999, *Nature*, 398, 368
- Nakamura, T., Mazzali, P. A., Nomoto, K., & Iwamoto, K. 2000, *ApJ*, submitted
- Nadyozhin, D. K. 1985, *Ap&SS*, 112, 225
- Norris, J. P., Bonnell, J. T. & Watanabe, K. 1999, *ApJ*, 518, 901

- Norris, J. P., Marani, G. F. & Bonnell, J. T. 2000, *ApJ*, 534, 248
- Ostriker, J. P., & McKee, C. F. 1988, *Rev. Mod. Phys.*, 60, 1
- Paczynski, B. 1998, *Gamma-Ray Bursts: 4th Huntsville Symposium*, eds. C.A. Meegan, R.D. Preece, & T.M. Koshut, Woodbury: New York
- Panaitescu, A., Mészáros, P. & Rees, M. J. 1998, *ApJ*, 503, 314
- Patat, F., & Piemonte, A. 1998 *IAU Circ.* 6918
- Pendleton, et al. 1997, *Gamma-Ray Bursts: 4th Huntsville Symposium*, eds. C.A. Meegan, R.D. Preece, & T.M. Koshut, Woodbury: New York
- Pian, E. & 27 colleagues 2000, *ApJ*, 536, 778
- Piran, T. 1999, *Physics Reports*, 314, 575
- Rees, M. J. & Mészáros, P. 1998, *ApJ*, 496, L1
- Reichart, D. E. 1999, *ApJ*, 521, 111
- Sakurai, A. 1960, *Comm. Pure Appl. Math.*, 13, 353
- Sari, R., & Piran, T. 1997, *MNRAS*, 287, 110
- Sari, R. & Mészáros, P. 2000, *ApJ*, 535, L33
- Schneid, E. J. et al. 1995, *ApJ*, 453, 95
- Sedov, L. I. 1946, *Prikl. Mat. Mekh.* 10, 241, No. 2
- Sedov, L. I. 1959, *Similarity & Dimensional Methods in Mechanics* (Academic, New York)
- Shapiro, P. R. 1979, *ApJ*, 233, 831
- Shaviv, N. J. & Dar, A. 1995, *ApJ*, 447, 863
- Smith, D. A., Hurley, K., & Cline, T. 2000, *GCN* 568
- Soffitta, P., et al. 1998, *IAUC* 6884
- Sollerman, J. et al. 2000, *ApJ*, 537, L127
- Springmann, U. 1994, *A&A*, 289, 505
- Taylor, G. I. 1950, *Proc. R. Soc. London*, 201, 159
- Thorsett, S. E., & Hogg, D. W. 1999, *GCN* 197
- Tinney, C., Stathakis, R., Cannon, R., & Galama, T.J. 1998, *IAUC* 6896
- Tkachenko, A. Y., Terekhov, O. V., Sunyaev, R. A., Burenin, R. A., Barat, C., Dezalay, J. -. & Vedrenne, G. 2000, *A&A*, 358, L41
- Turatto, M. et al. 2000, *ApJ*, 534, L57
- Wang, L. & Wheeler, J. C. 1998, *ApJ*, 504, L87
- Wang, L., Howell, D. A., Hoefflich, P., & Wheeler, J. C. 2000, *ApJ*, submitted, astro-ph/9912033
- Waxman, E., & Loeb, A. 1999, *ApJ*, 515, 721
- Waxman, E., & Draine, B. T. 2000, *ApJ*, 537, 796
- Weaver, T. A. 1976, *ApJS*, 32, 233
- Weiler, K. W., Panagia, N., Sramek, R. A., Van Dyk, S. D., Montes, M. J., & Lacey, C. K. 2000, in *The Largest Explosions Since the Big Bang: Supernovae and Gamma Ray Bursts, 1999 STScI May Symposium*, astro-ph/0002501
- Wheeler, J. C., Yi, I., Hoefflich, P., & Wang, L. 2000, *ApJ*, 537, 810
- Wheeler, J. C., Hoefflich, P., Wang, L., & Yi, I. 2000, in *Gamma-Ray Bursts: 5th Huntsville Symposium*, astro-ph/9912080
- Wieringa, M. H., Kulkarni, S. R. & Frail, D. A. 1999, *A&AS*, 138, 467
- Woosley, S. E. 1993, *ApJ*, 405, 273
- Woosley, S. E., & Weaver, T. A. 1986, *ARA&A*, 24, 205
- Woosley, S. E., & Baron, E. 1992, *ApJ*, 391, 228
- Woosley, S. E., Eastman, R. G., & Schmidt, B. P. 1999, *ApJ*, 516, 788

This 2-column preprint was prepared with the AAS L^AT_EX macros v5.0.